Journal of Sound and Vibration (1998) **210**(4), 483–515

PRINCIPAL RESPONSE OF DUFFING OSCILLATOR TO COMBINED DETERMINISTIC AND NARROW-BAND RANDOM PARAMETRIC EXCITATION

H. Rong, W. Xu and T. Fang

Institute of Vibration Engineering, Northwestern Polytechnical University, Xi'an 710072, *China*

(*Received* 11 *December* 1996, *and in final form* 9 *September* 1997)

The principal resonance of a Duffing oscillator to combined deterministic and narrow-band random parametric excitations is investigated. In particular, the case in which the parametric terms share close frequencies is examined. The method of multiple scales is used to determine the equations of modulation of amplitude and phase. The behavior, stability and bifurcation of steady state response are studied by means of qualitative analyses. Jumps are shown to occur if the random excitation is small. The effects of damping, detuning, and magnitudes of deterministic and narrow-band parametric excitations are analyzed. The theoretical analyses are verified by numerical results.

1. INTRODUCTION

Most physical excitations exhibit a randomly fluctuating character and contain a wide spectrum of frequencies, which may result in severe vibrations. Due to the highly unpredictable trends of these natural hazard excitations, it is necessary to have some stochastic formulations to describe them. As they can be fully characterized by probability density functions or certain statistical measures, the method of random vibrations has a wide range of applications to practical engineering problems.

However, most of the researchers in our field concentrate their attention on the response of system only under random external excitation. There are many phenomena in which parametric and self-excited vibrations interact with one another. Examples are flow-induced vibrations and vibrations in rotor systems. So, the study of the random parametric excited systems are more important than that of random external excited ones, and are theoretically more difficult especially when the excitations are narrow-band random processes [1]. In the case when the systems are excited by combined deterministic harmonic and wide-band random processes, Stratonovitch and Romanoviskii [2], Dimentberg *et al*. [3], and Namachchivaya [4] used the method of random averaging and Khasminskii to investigate the almost certain stability of the system. The moment stability was discussed by Ariaratnam and Tam [5], and Dimentberg [6] investigated the response of the systems. Until now, the analyses of the responses and stability of non-linear systems under combined deterministic and narrow-band random excitation have not been investigated.

In this paper, the principal resonance of a Duffing oscillator to combined deterministic and narrow-band random parametric excitations is investigated. In particular, the case in

0022–460X/98/090483 + 33 $25.00/0/sv971325

which the parametric terms share close frequencies is examined. The method of multiple scales is used to determine the equations of modulation of amplitude and phase. The behavior, stability and bifurcation of steady state response are studied by means of qualitative analyses. Jumps are shown to occur if the random excitation is small. The effects of damping, detuning, and magnitudes of deterministic and narrow-band parametric excitations are analyzed. The theoretical analyses are verified by numerical results.

2. GENERAL ANALYSIS

Consider the Duffing oscillator under combined deterministic and narrow-band random parametric excitations

$$\ddot{u} + \varepsilon\beta\dot{u} + \omega^2(u + \varepsilon\alpha u^3) + \varepsilon(\xi(t) + h_0 \cos \Omega_0 t + k_0 \sin \Omega_0 t)u = 0, \tag{1}$$

where dots indicate differentiation with respect to the time t, ε is a small parameter, β and ω are stiffness coefficient and natural frequency respectively, α represents the density of the non-linear term, h_0 and k_0 are constants, Ω_0 is the frequency of the deterministic harmonic excitations, and $\xi(t)$ is a narrow-band random process which is governed by the following equation:

$$\xi(t) = h_1 \cos \Omega_1 t + k_1 \sin \Omega_1 t, \tag{2}$$

where $h_1 = h_1(\varepsilon t)$, $k_1 = k_1(\varepsilon t)$ are slowly varying stationary random processes with zero means. Model (2) represents a wide kind of narrow-band random excitation. For example, the zero-mean Gaussian narrow-band random process could be obtained by filtering a white noise through a linear filter [7]

$$\ddot{\xi} + \gamma\dot{\xi} + \Omega_1^2\xi = \sqrt{\gamma}\Omega_1 W, \tag{3}$$

where Ω_1 is the center frequency of $\xi(t)$ and γ is the bandwidth of the filter. The autocorrelation function of the white noise W is given by

$$R_W(\tau) = 2\pi S_0 \delta(\tau), \tag{4}$$

where S_0 is the spectrum constant of W and δ is Dirac delta function. The spectrum density function of $\xi(t)$ given by equation (3) is

$$\frac{\gamma\Omega_1^2 S_0}{(\Omega_1^2 - \omega^2)^2 + \omega^2\gamma^2} \to \pi S_0 \delta(\Omega_1), \qquad \gamma \to 0.$$

Substituting equation (2) into equation (3) and performing deterministic and stochastic averaging of the equations for the modulations of h_1 and k_1 [8, 9], one obtains

$$\begin{cases} \dot{h}_1 + \dfrac{\gamma}{2} h_1 = \sqrt{\dfrac{\gamma}{2}}\, W_1 \\[2ex] \dot{k}_1 + \dfrac{\gamma}{2} k_1 = \sqrt{\dfrac{\gamma}{2}}\, W_2. \end{cases} \tag{5}$$

The white noise components W_1 and W_2 are independent and their autocorrelation functions are given by equation (4). The autocorrelation functions of h_1 and k_1 are

$$R_{h_1}(\tau) = R_{k_1}(\tau) = \pi S_0 \exp(-\tfrac{1}{2}\gamma|\tau|). \tag{6}$$

The correlation time of h_1 and k_1 is of $o(1/\gamma)$. This means that for a sufficiently small value of γ, h_1 and k_1 are slowly varying functions of time.

The method of multiple scales [10] has been widely used in the analysis of deterministic systems. Rajan and Davies [8], Nayfeh and Serhan [9] extend this method to the analysis of non-linear systems under random external excitations. In this paper, the multiple scale method is used to investigate the response and stability of system (1). Then, a uniformly approximate solution of equation (1) is sought in the form

$$u(t, \varepsilon) = u_0(T_0, T_1) + \varepsilon u_1(T_0, T_1) + \cdots, \tag{7}$$

where $T_0 = t$ is a fast scale and $T_1 = \epsilon t$ is a slow scale.

Since h_1 and k_1 are slowly varying functions of time, one obtains

$$h_1 = h_1(T_1), \qquad k_1 = k_1(T_1).$$

By denoting $D_0 = \partial/\partial T_0$ and $D_1 = \partial/\partial T_1$, the ordinary-time derivatives can be transformed into partial derivatives as

$$\frac{\mathrm{d}}{\mathrm{d}t} = D_0 + \varepsilon D_1, \qquad \frac{\mathrm{d}^2}{\mathrm{d}t^2} = D_0^2 + 2\varepsilon D_0 D_1.$$

Substituting equation (7) into equation (1) and equating coefficients of like powers of ε, one obtains

$$D_0^2 u_0 + \omega^2 u_0 = 0, \tag{8}$$

$$D_0^2 u_1 + \omega^2 u_1 = -2D_0 D_1 u_0 - \beta D_0 D_1 u_0 - (\xi(t) + h_0 \cos \Omega_0 t + k_0 \sin \Omega_0 t)u_0 - \alpha\omega^2 u_0^3. \tag{9}$$

The general solution of equation (8) can be written as

$$u_0(T_0, T_1) = A(T_1)\exp(i\omega T_0) + cc, \tag{10}$$

where cc represents the complex conjugate of its preceding term, and $A(T_1)$ is the slowly varying amplitude of the response. Hence, equation (9) becomes

$$\begin{aligned} D_0^2 u_1 + \omega^2 u_1 = &-2i\omega A' \exp(i\omega T_0) - i\omega\beta A \exp(i\omega T_0) \\ &- \alpha\omega^2 A^3 \exp(3i\omega T_0) - 3\alpha\omega^2 A^2 \bar{A} \exp(i\omega T_0) \\ &- \frac{A}{2}(h_0 - ik_0)\exp[i(\Omega_0 + \omega)T_0] - \frac{\bar{A}}{2}(h_0 - ik_0)\exp[i(\Omega_0 - \omega)T_0] \\ &- \frac{A}{2}(h_1 - ik_1)\exp[i(\Omega_1 + \omega)T_0] - \frac{\bar{A}}{2}(h_1 - ik_1)\exp[i(\Omega_1 - \omega)T_0] + cc, \end{aligned} \tag{11}$$

where the prime stands for the derivative with respect to T_1 and the overbar stands for the complex conjugate. Any particular solution of equation (11) contains secular terms, which are generated by the first, second and fourth terms on the right-hand side of equation (11). Moreover, it may contain small-divisor terms dependent on the resonance conditions. From the sixth and eighth terms on the right-hand side of equation (11), it is clear that resonance occurs when $\Omega_0 \approx 2\omega$, or $\Omega_1 \approx 2\omega$, or both conditions apply. In what follows we shall investigate the principal resonances of the system (1), in which Ω_0 and Ω_1 are either far apart or close to each other.

3. PRINCIPAL PARAMETRIC RESONANCE I

Here we consider the case of principal resonance when $\Omega_0 \approx 2\omega$ but Ω_1 is far from Ω_0. Introducing the detuning parameter σ as follows

$$\Omega_0 = 2\omega + \varepsilon\sigma, \tag{12}$$

one has

$$(\Omega_0 - \omega)T_0 = \omega T_0 + \sigma T_1.$$

Using the above equation, we can transform the small-divisor term which arises from $\exp[i(\Omega_0 - \omega)T]$ in equation (11) into a secular term. Then, eliminating the secular terms yields

$$2i\omega A' + i\beta\omega A + 3\alpha\omega^2 A^2 \bar{A} + \tfrac{1}{2}\bar{A}(h_0 - ik_0)\exp(i\sigma T_1) = 0. \tag{13}$$

Expressing A in the polar form

$$A(T_1) = a(T_1)\exp[i\varphi(T_1)]. \tag{14}$$

Substituting equation (14) into equation (13) and separating the real and imaginary parts of equation (13), one obtains

$$\begin{cases} a' = -\dfrac{\beta}{2}a + \dfrac{a}{4\omega}(k_0 \cos\eta - h_0 \sin\eta) \\ a\eta' = \sigma a - 3\alpha\omega a^3 - \dfrac{a}{2\omega}(h_0\cos\eta + k_0\sin\eta), \end{cases} \tag{15}$$

where $\eta = \sigma T_1 - 2\varphi$. Equations (15) are the first-order equations governing the modulation of amplitude and phase. After solving a and η from these equations, the first-order uniform expansion of the solution of equation (1) is given by

$$\begin{aligned} u &= A(T_1)\exp(i\omega T_0) + cc + O(\varepsilon) \\ &= a\exp\left[i\left(\omega T_0 + \frac{\sigma}{2}T_1 - \frac{\eta}{2}\right)\right] + cc + O(\varepsilon) \\ &= a\exp\left[i\left(\frac{\Omega_0}{2}t - \frac{\eta}{2}\right)\right] + cc + O(\varepsilon) \\ &= 2a(\varepsilon t)\cos\left[\frac{\Omega_0}{2}t - \frac{\eta(\varepsilon t)}{2}\right] + O(\varepsilon). \end{aligned} \tag{16}$$

3.1. STEADY SOLUTIONS AND THEIR STABILITY

It is obvious that equations (15) have a solution $a = 0$, which corresponds to the trivial steady state response. Non-trivial steady state responses correspond to the non-trivial fixed points of equations (15). That is, they satisfy $a' = 0$, $\eta' = 0$, $a \neq 0$, and are given by

$$\begin{cases} \beta = \dfrac{1}{2\omega}(k_0\cos\eta - h_0\sin\eta) \\ \sigma - 3\alpha\omega a^2 = \dfrac{1}{2\omega}(h_0\cos\eta + k_0\sin\eta). \end{cases} \tag{17}$$

Eliminating $\sin\eta$ and $\cos\eta$ from equations (17) yields the frequency response relation

$$a = \frac{1}{\sqrt{\omega}}\left[\frac{\sigma}{3\alpha} \pm \frac{1}{3\alpha}\sqrt{\frac{h_0^2 + k_0^2 - 4\omega^2\beta^2}{4\omega^2}}\right]^{1/2}. \tag{18}$$

It can be shown that non-trivial steady state solutions exist, at most, in a finite interval of the detuning parameter σ. Indeed, from (18) the region of existence of non-trivial steady state response is given as follows

$$h_0^2 + k_0^2 > 4\omega^2\beta^2, \tag{19}$$

when $\alpha > 0$, and

$$\sigma < \sqrt{\frac{h_0^2 + k_0^2 - 4\omega^2\beta^2}{4\omega^2}}, \tag{20}$$

there is a trivial steady state response, together with a non-trivial steady state response whose stability needs further investigation. When $\alpha > 0$, and

$$\sigma > \sqrt{\frac{h_0^2 + k_0^2 - 4\omega^2\beta^2}{4\omega^2}}, \tag{21}$$

there is a trivial steady state response together with two non-trivial steady state responses which may be stable or unstable.

Only stable responses can be observed in the number simulation. To determine the stability of the trivial steady state response, it is convenient to rewrite A in the form

$$A = (x + iy)\exp(i\sigma T_1/2). \tag{22}$$

Then equation (13) is equivalent to the following equations

$$\begin{cases} x' = \left(-\dfrac{\beta}{2} + \dfrac{k_0}{4\omega}\right)x + \left(\dfrac{\sigma}{2} + \dfrac{h_0}{4\omega}\right)y - \frac{3}{2}\alpha\omega(x^2 + y^2)y \\ \\ y' = \left(-\dfrac{\sigma}{2} + \dfrac{h_0}{4\omega}\right)x + \left(-\dfrac{\beta}{2} - \dfrac{k_0}{4\omega}\right)y + \frac{3}{2}\alpha\omega(x^2 + y^2)x. \end{cases} \tag{23}$$

The stability of the trivial solution $A = 0$ of equation (13) is the same as that of equation (23). The linearization of equation (23) at (0, 0) is

$$\begin{cases} x' = \left(-\dfrac{\beta}{2} + \dfrac{k_0}{4\omega}\right)x + \left(\dfrac{\sigma}{2} + \dfrac{h_0}{4\omega}\right)y \\ \\ y' = \left(-\dfrac{\sigma}{2} + \dfrac{h_0}{4\omega}\right)x + \left(-\dfrac{\beta}{2} - \dfrac{k_0}{4\omega}\right)y. \end{cases} \tag{24}$$

The eigenvalues of the coefficient matrix of equations (24) are

$$\lambda_{1,2} = -\frac{\beta}{2} \pm \frac{1}{4\omega}\sqrt{h_0^2 + k_0^2 - 4\sigma^2\omega^2}. \tag{25}$$

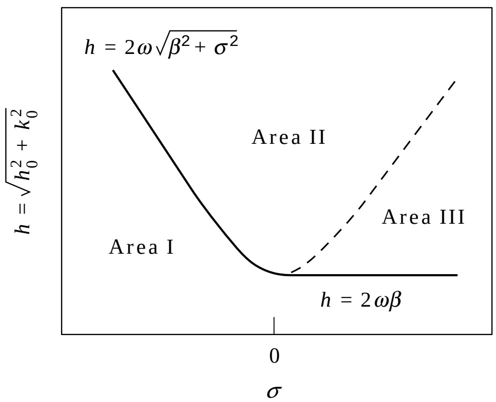

Figure 1. The parameter area of the steady state solution.

The trivial solution is asymptotically stable if the real parts of λ_i ($i = 1, 2$) are less than zero, and it is unstable if at least one of the real parts of λ_i is larger than zero. As a result, we conclude that the trivial solution of equations (23) is stable if and only if

$$h_0^2 + k_0^2 < 4\omega^2(\beta^2 + \sigma^2). \tag{26}$$

To determine the stability of the non-trivial steady state responses given by (18), equations (15) are used. Let

$$a = a_0 + a_1, \qquad \eta = \eta_0 + \eta_1, \tag{27}$$

where (a_0, η_0) is given by (17), and a_1, η_1 are perturbation terms. Substituting equations (27) into equations (15) and neglecting the non-linear terms, one obtains the linearization of the modulation equations (15) at (a_0, η_0)

$$\begin{cases} a_1' = -\dfrac{a_0}{4\omega}(k_0 \sin\eta_0 + h_0 \cos\eta_0)\eta_1 \\[2ex] \eta_1' = -6\alpha\omega a_0\, a_1 - \dfrac{1}{2\omega}(k_0 \cos\eta_0 - h_0 \sin\eta_0)\eta_1. \end{cases} \tag{28}$$

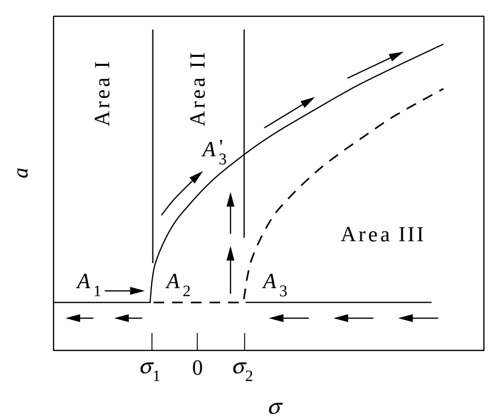

Figure 2. Frequency response of Duffing system: ——, stable solution; –––, unstable solution.

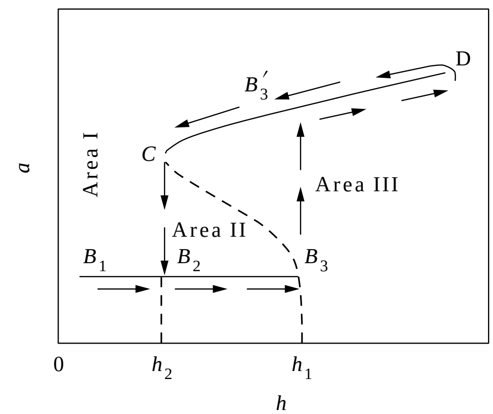

Figure 3. Response of Duffing system: ——, stable solution; –––, unstable solution.

The eigenvalues of the coefficient matrix of equations (28) are

$$\lambda_{1,2} = -\frac{\beta}{2} \pm \tfrac{1}{2}\sqrt{\beta^2 + 6\alpha a_0^2(h_0 \cos\eta_0 + k_0 \sin\eta_0)}. \tag{29}$$

If $(h_0 \cos\eta_0 + k_0 \sin\eta_0)$ is positive, the non-trivial steady state solutions of equations (15) are always unstable. From equations (17) one obtains

$$h_0 \cos\eta_0 + k_0 \sin\eta_0 = 2\omega(\sigma - 3\alpha\omega a_0^2).$$

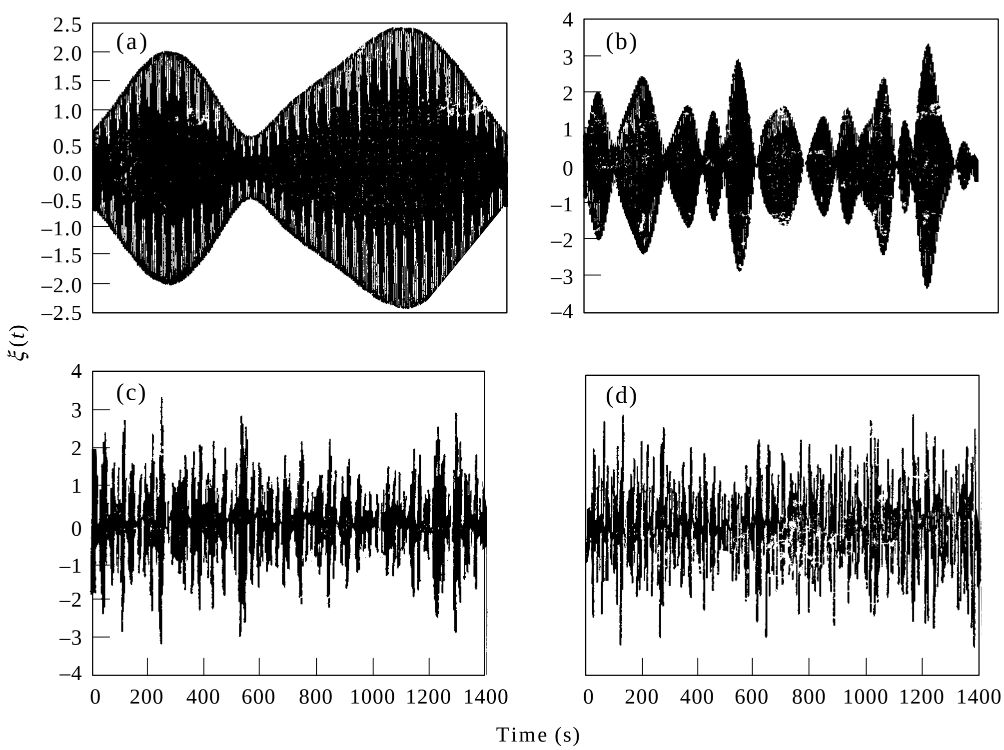

Figure 4. Time history of $\xi(t)$. (a) $\gamma = 0{\cdot}02$; (b) $\gamma = 0{\cdot}1$; (c) $\gamma = 0{\cdot}5$; (d) $\gamma = 1{\cdot}0$.

So, if equations (19) and (20) both take place, equations (15) may have one stable non-trivial steady state solution, and if equations (19) and (21) both hold, equations (15) would have two possible non-trivial steady state solutions, from which the larger one is stable and the smaller one unstable.

Above all, according to the detuning parameter σ and the amplitude of the deterministic harmonic excitation $h = \sqrt{h_0^2 + k_0^2}$, the stability area of steady state solution of equations (15) can be divided into the following three parts, as shown in Figure 1,

$$\text{area I} = \{(\sigma, h)\colon \sigma < 0, h < 2\omega\sqrt{\beta^2 + \sigma^2}\} \cup \{(\sigma, h)\colon \sigma > 0, h < 2\omega\beta\},$$

$$\text{area II} = \{(\sigma, h)\colon h > 2\omega\sqrt{\beta^2 + \sigma^2}\},$$

$$\text{area III} = \{(\sigma, h)\colon \sigma > 0, 2\omega\beta < h < 2\omega\sqrt{\beta^2 + \sigma^2}\}.$$

In area I, only the trivial steady state solution is stable and so the response of equation (1) will converge to zero for any initial value when $t \to \infty$. In area II, only the non-trivial steady state solution is stable and so the response of equation (1) will converge to this non-trivial solution for any non-trivial initial value when $t \to \infty$. In area III, the trivial steady state solution and the larger steady state solution are stable so the response of equation (1) may converge to zero or the larger steady state solution for different initial values.

3.2. BIFURCATIONS OF STEADY STATE RESPONSE AND JUMPS

If σ is chosen to be a bifurcation parameter and the intensity of deterministic harmonic excitation $h = \sqrt{h_0^2 + k_0^2} > 2\omega\beta$ as a constant, when σ increases from a small value, the

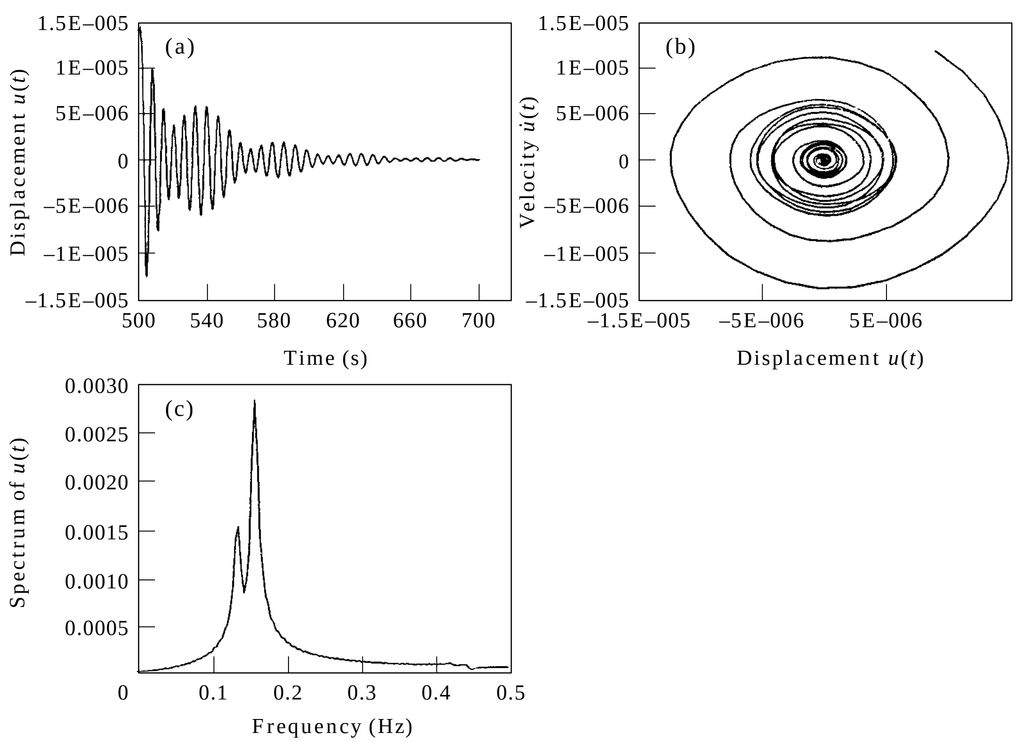

Figure 5. Numerical results of equation (1): $\Omega_0 = 1{\cdot}8$, $\Omega_1 = 10{\cdot}0$, $h_0 = k_0 = 2{\cdot}0$, $\sigma_\xi^2 = 1{\cdot}0$. (a) Time history of $u(t)$; (b) phase plot; (c) spectrum with frequency of $u(t)$.

variation of steady state response with σ is shown in Figure 2 along $A_1 \rightarrow A_2 \rightarrow A_3'$. At the point A_2, i.e., when

$$\sigma = \sigma_1 = -\sqrt{\frac{h^2 - 4\omega^2\beta^2}{4\omega^2}} = -\sqrt{\frac{h_0^2 + k_0^2 - 4\omega^2\beta^2}{4\omega^2}}, \tag{30}$$

the steady state response turns from a trivial one to a non-trivial one when σ increases; so σ_1 is a bifurcation point. When σ decreases from a large value, the variation of steady state response with σ is shown in Figure 2 along $A_3 \rightarrow A_3' \rightarrow A_2 \rightarrow A_1$. At the point A_3, i.e., when

$$\sigma = \sigma_2 = \sqrt{\frac{h^2 - 4\omega^2\beta^2}{4\omega^2}} = \sqrt{\frac{h_0^2 + k_0^2 - 4\omega^2\beta^2}{4\omega^2}}, \tag{31}$$

the steady state response will jump from A_3 to A_3', so σ_2 is also a steady state response bifurcation point.

If h is chosen as a bifurcation parameter and $\sigma > 0$ as a constant, when h increases from a small value, the variation of steady state response with h is shown in Figure 3. At the point B_3, i.e., when

$$h = h_1 = 2\omega\sqrt{\beta^2 + \sigma^2}, \tag{32}$$

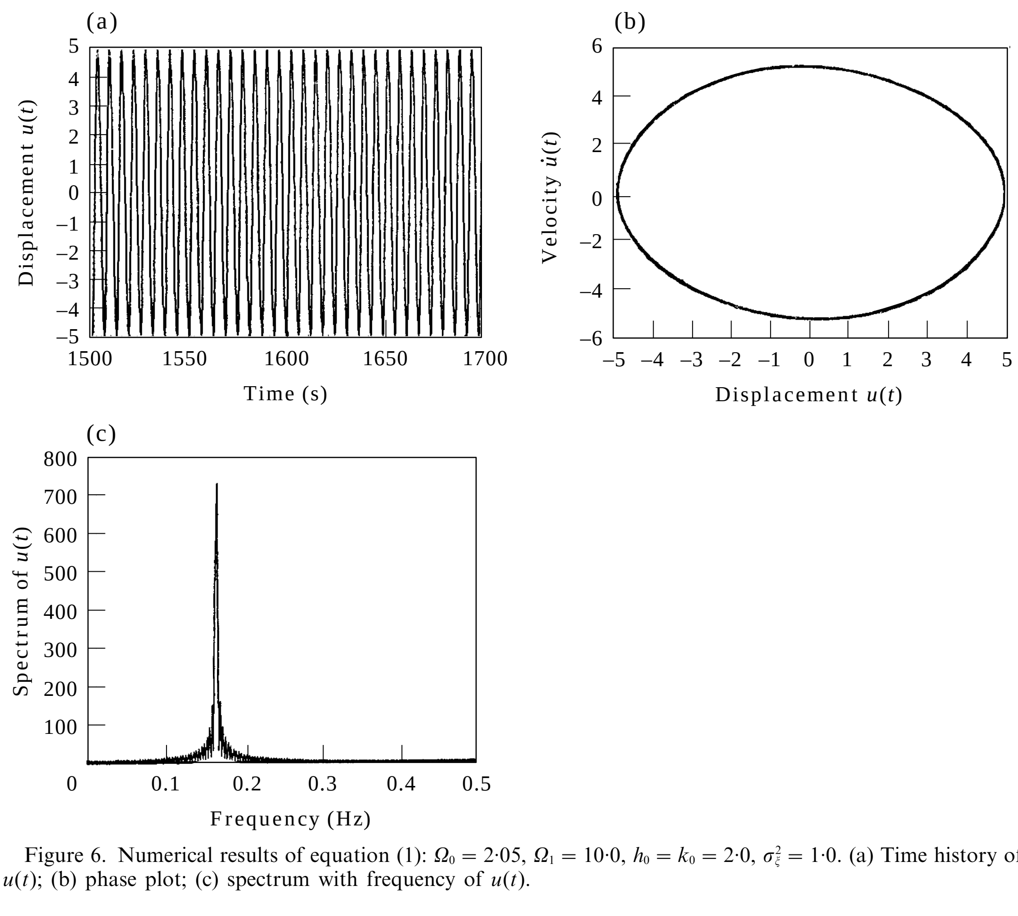

Figure 6. Numerical results of equation (1): $\Omega_0 = 2{\cdot}05$, $\Omega_1 = 10{\cdot}0$, $h_0 = k_0 = 2{\cdot}0$, $\sigma_\xi^2 = 1{\cdot}0$. (a) Time history of $u(t)$; (b) phase plot; (c) spectrum with frequency of $u(t)$.

the steady state response will jump from B_3 to B_3'. When h decreases from a large value, the variation of steady state response with h is shown in Figure 3 through $D \rightarrow B_3' \rightarrow C$. At point C, i.e., when

$$h = h_2 = 2\omega\beta, \tag{33}$$

the steady state response will jump from C to B_2, so h_1 and h_2 are also bifurcation points.

3.3. NUMERICAL SIMULATION

In the theoretical analyses above, the narrow-band random excitation $\xi(t)$ can be modelled by equation (2) or (3). For numerical simulation it is more convenient to use the pseudorandom signal given by [8, 11]

$$\xi(t) = \sqrt{\frac{2\sigma_\xi^2}{N}} \sum_{k=1}^{N} \cos(\omega_k t + \varphi_k). \tag{34}$$

The frequency ω_k is chosen independently from a random population with probability density function which is the same as the spectrum of $\xi(t)$, and the random phases φ_k's are independent and uniformly distributed in $(0, 2\pi)$. Shinozuka [11] has shown that $\xi(t)$ tends to a Gaussian process as $N \rightarrow \infty$. For the very narrow-band simulations used here, the spectrum chosen is a simple top-hat type, and the random frequencies ω_k's are

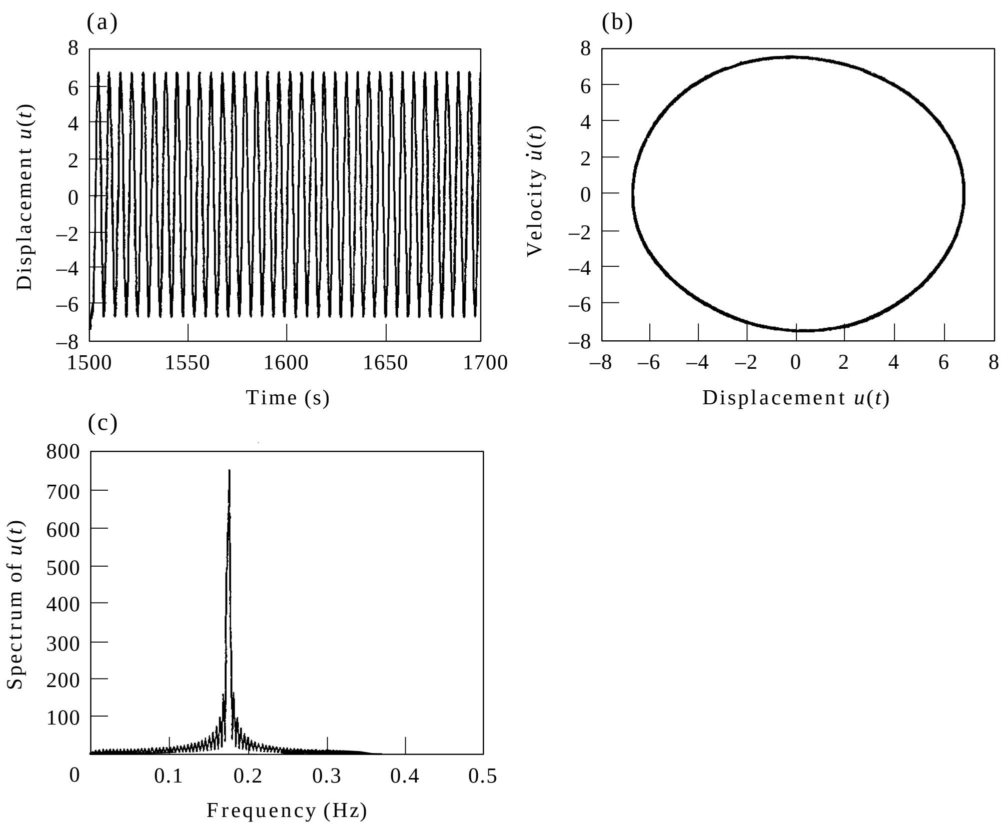

Figure 7. Numerical results of equation (1): $\Omega_0 = 2{\cdot}2$, $\Omega_1 = 10{\cdot}0$, $h_0 = k_0 = 2{\cdot}0$, $\sigma_\xi^2 = 1{\cdot}0$, $u(0) = -2{\cdot}2$, $\dot{u}(0) = 2{\cdot}0$. (a) Time history of $u(t)$; (b) phase plot; (c) spectrum with frequency of $u(t)$.

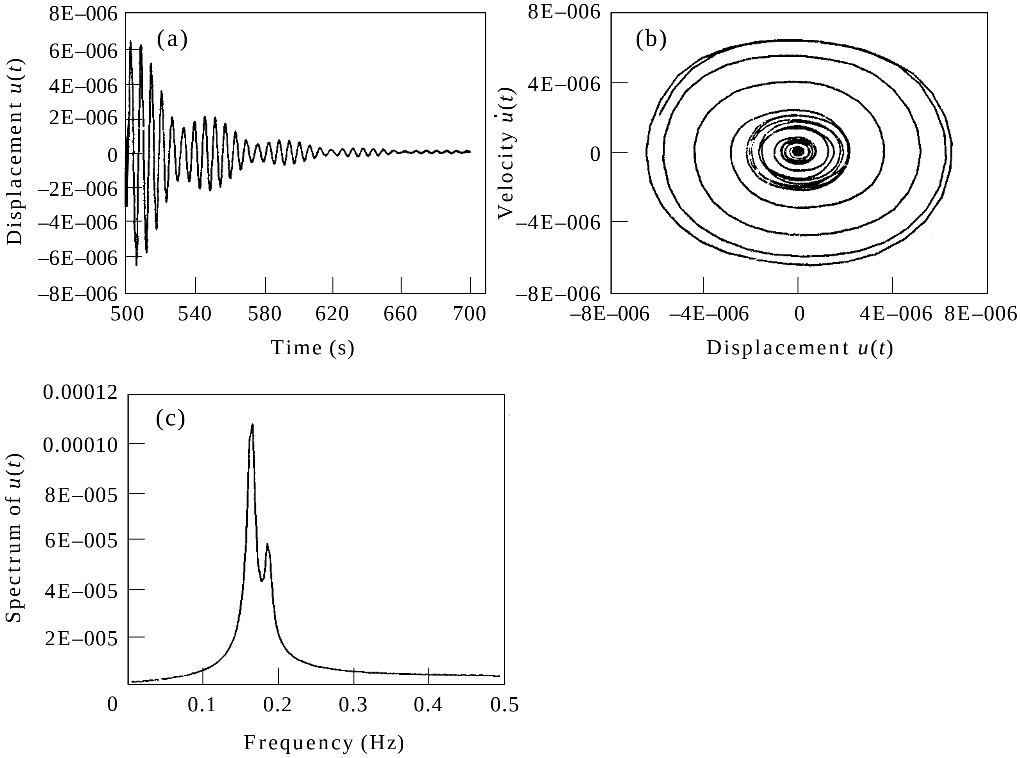

Figure 8. Numerical results of equation (1): $u(0) = 1{\cdot}1$, $\dot{u}(0) = 1{\cdot}1$ (other parameters are the same as in Figure 7). (a) Time history of $u(t)$; (b) phase plot; (c) spectrum with frequency of $u(t)$.

distributed uniformly in $(\Omega_1 - \gamma/2, \Omega_1 + \gamma/2)$. When N is large enough, Rajan and Davies [8] show

$$E\xi^2(t) = \sigma_\xi^2, \qquad E\xi^4(t) = 3\sigma_\xi^4.$$

In the numerical simulation, the parameters in systems (1) and (34) are chosen as follows: $N = 500$, $\gamma = 0{\cdot}1$, $\varepsilon = 0{\cdot}1$, $\beta = 0{\cdot}5$, $\alpha = 0{\cdot}1$, and $\omega = 1{\cdot}0$.

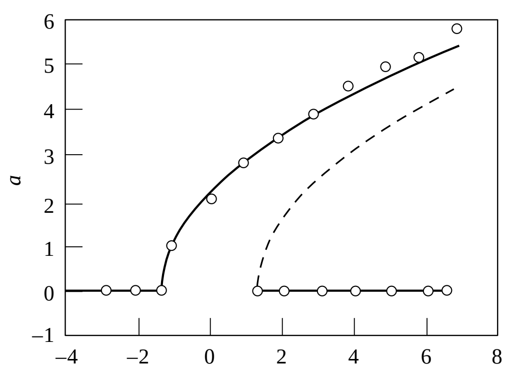

Figure 9. Frequency response of Duffing system: $h_0 = k_0 = 2{\cdot}0$, $\Omega_1 = 10{\cdot}0$, $\sigma_\xi^2 = 1{\cdot}0$. ——, Stable solution; ---, unstable solution; ○○○, numerical solution.

The time history of the narrow-band random excitation $\xi(t)$ defined by equation (34) is shown in Figure 4. The governing equation (1) is numerically integrated by the fourth order Runge–Kutta algorithm, and the numerical results are shown in Figures 5–8. In Figure 5, the parameters (σ, h) are in area I, so the steady state response is a trivial solution. In Figure 6, the parameters (σ, h) are in area II, so the steady state response is a non-trivial solution. In Figures 7 and 8, the parameters (σ, h) are in area III, so the steady state response may tend to the trivial solution (Figure 7) or to the non-trivial solution (Figure 8), depending on the initial values. Jumps are also observed in the simulation. The variations of the steady state response with σ is shown in Figure 9. The variations of the steady state response with h are shown in Figure 10.

4. PRINCIPAL PARAMETRIC RESONANCE II

Here, the case of principal parametric resonance is considered when $\Omega_1 \approx 2\omega$ but Ω_0 is far from Ω_1. Introducing the detuning parameter σ as follows

$$\Omega_1 = 2\omega + \varepsilon\sigma, \tag{35}$$

one has

$$(\Omega_1 - \omega)T_0 = \omega T_0 + \sigma T_1.$$

Using the above equation, the small-divisor term which arise from $\exp[i(\Omega_1 - \omega)T]$ in equation (11) can be transformed into a secular term. Then, eliminating the secular term yields

$$2i\omega A' + i\beta\omega A + 3\alpha\omega^2 A^2 \bar{A} + \tfrac{1}{2}\bar{A}[h_1(T_1) - ik_1(T_1)]\exp(i\sigma T_1) = 0. \tag{36}$$

4.1. STEADY SOLUTIONS AND THEIR STABILITY

Substituting equation (22) into equation (36) and separating the real and imaginary parts of equation (36), one obtains

$$\begin{cases} x' = \left(-\dfrac{\beta}{2} + \dfrac{k_1}{4\omega}\right)x + \left(\dfrac{\sigma}{2} + \dfrac{h_1}{4\omega}\right)y - \tfrac{3}{2}\alpha\omega(x^2 + y^2)y \\[2ex] y' = \left(-\dfrac{\sigma}{2} + \dfrac{h_1}{4\omega}\right)x + \left(-\dfrac{\beta}{2} - \dfrac{k_1}{4\omega}\right)y + \tfrac{3}{2}\alpha\omega(x^2 + y^2)x. \end{cases} \tag{37}$$

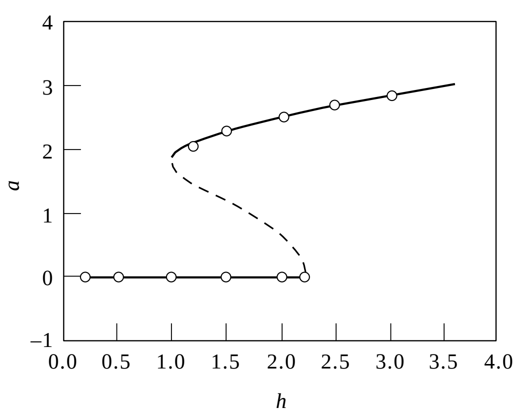

Figure 10. Response of Duffing system: $\Omega_1 = 10{\cdot}0$, $\sigma_\xi^2 = 1{\cdot}0$, $\sigma = 1{\cdot}0$. ——, Stable solution; – – –, unstable solution; ○○○, numerical solution.

The stochastic Lyapunov function can be constructed as follows

$$V(T_1) = x^2(T_1) + y^2(T_1).$$

From equations (37) one has

$$V' = -\beta V + \frac{1}{2\omega}(k_1 x^2 + 2h_1 xy - k_1 y^2) \leqslant \left(-\beta + \frac{|h_1| + |k_1|}{2\omega}\right)V,$$

which yields

$$V(T) \leqslant V(0)\exp\left[\int_0^T \left(-\beta + \frac{|h_1(T_1)| + |k_1(T_1)|}{2\omega}\right)\mathrm{d}T_1\right]. \tag{38}$$

For ergodic random processes h_1 and k_1 and large enough t, one obtains

$$\frac{1}{T}\int_0^T \left(-\beta + \frac{|h_1(T_1)| + |k_1(T_1)|}{2\omega}\right)\mathrm{d}T_1 \to -\beta + \frac{1}{2\omega}(E|h_1| + E|k_1|),$$

with probability one. From the above equation and equation (38), it can be concluded that if there exists some positive number $\varepsilon_1 > 0$, such that

$$-\beta + \frac{1}{2\omega}(E|h_1| + E|k_1|) < -\varepsilon_1, \tag{39}$$

then $V(T)$ will tend to zero while $T \to \infty$, so that the trivial solution of equations (37) is almost certainly stable. If only the second moments of h_1 and k_1, are known by Schwarz inequality the sufficient almost certain stability condition of the trivial solution of equations (37) can be obtained as follows

$$E(h_1^2 + k_1^2) < 2\omega^2\beta^2.$$

From equation (5) one has

$$Eh_1^2 = Ek_1^2 = E\xi^2(t) = \sigma_\xi^2,$$

hence the sufficient almost certain stability condition can be rewritten as

$$\sigma_\xi^2 < \omega^2\beta^2. \tag{40}$$

To obtain the necessary and sufficient almost certain stability condition of equations (37), its linearized equation is considered in the neighborhood of (0, 0).

$$\begin{cases} x' = \left(-\dfrac{\beta}{2} + \dfrac{k_1}{4\omega}\right)x + \left(\dfrac{\sigma}{2} + \dfrac{h_1}{4\omega}\right)y \\[2ex] y' = \left(-\dfrac{\sigma}{2} + \dfrac{h_1}{4\omega}\right)x + \left(-\dfrac{\beta}{2} - \dfrac{k_1}{4\omega}\right)y. \end{cases} \tag{41}$$

For ergodic random processes h_1 and k_1, according to Oseledec multiplicative ergodic theorem [12], it can be concluded that for any initial value (x_0, y_0) the Lyapunov exponent of the solution $(x(T_1, x_0), y(T_1, y_0))$ of equations (41) is

$$\lambda(x_0, y_0) = \lim_{T_1 \to \infty} \frac{1}{T_1} \ln\sqrt{x^2(T_1, x_0) + y^2(T_1, y_0)}, \qquad w.p.1 \tag{42}$$

and $\lambda(x_0, y_0)$ can take only the following deterministic values

$$\lambda_{min} = \lambda_2 < \lambda_1 = \lambda_{max}.$$

So the almost certain stability of the trivial solution (41) can be determined by the largest Lyapunov exponent $\lambda = \lambda_{max}$, i.e., when $\lambda < 0$ the trivial solution is almost certainly stable and when $\lambda > 0$ the trivial one is unstable.

By the following transformation

$$x = a\cos\frac{\eta}{2}, \quad y = -a\sin\frac{\eta}{2}, \quad \rho = \ln a, \qquad a \neq 0, \tag{43}$$

equations (41) can be rewritten as

$$\begin{cases} a' = -\dfrac{\beta}{2}a + \dfrac{a}{4\omega}(k_1\cos\eta - h_1\sin\eta) \\ \eta' = \sigma - \dfrac{1}{2\omega}(h_1\cos\eta + k_1\sin\eta) \\ \rho' = -\dfrac{\beta}{2} + \dfrac{1}{4\omega}(k_1\cos\eta - h_1\sin\eta). \end{cases} \tag{44}$$

Then the largest Lyapunov exponent is

$$\lambda = -\frac{\beta}{2} + \frac{1}{4\omega}\lim_{T\to\infty}\frac{1}{T}\int_0^T [k_1(T_1)\cos\eta(T_1) - h_1(T_1)\sin\eta(T_1)]\,\mathrm{d}T_1. \tag{45}$$

4.2. NON-TRIVIAL STEADY STATE RESPONSE

For small intensities of random excitation the values of h_1 and k_1 are small, and so from equation (45) it is obvious that the largest Lyapunov exponent of equations (41) is less than 0, i.e., the trivial steady state response is stable. When σ_ξ^2 of the random excitation increases, the trivial steady state solution will become unstable and so there will be a non-trivial steady state solution. To obtain the probability characteristic of the non-trivial steady state solution, by transformation (14) we rewrite equation (36) as

$$\begin{cases} a' = -\dfrac{\beta}{2}a + \dfrac{a}{4\omega}(k_1\cos\eta - h_1\sin\eta) \\ \eta' = \sigma - 3\alpha\omega a^2 - \dfrac{1}{2\omega}(h_1\cos\eta + k_1\sin\eta). \end{cases} \tag{46}$$

Then the first order approximate solution of equation (1) is

$$u = 2a(\varepsilon t)\cos\left[\frac{\Omega_1}{2}t - \frac{\eta(\varepsilon t)}{2}\right] + O(\varepsilon).$$

By the averaging technique, equations (46) can be reduced to

$$\begin{cases} a' = -\dfrac{\beta}{2}a + \dfrac{a}{4\omega}h\cos\theta \\ \theta' = \sigma - 3\alpha\omega a^2 - \dfrac{h}{2\omega}\sin\theta, \end{cases} \tag{47}$$

where

$$\theta = \arctan \frac{k_1}{h_1} + \eta, \qquad h = \sqrt{h_1^2 + k_1^2}.$$

The temporal average over a fundamental period $2\pi/\Omega_1$ is implied here. The term $(\arctan k_1/h_1)'$ has been set to zero.

Since it is difficult to solve equations (17) exactly, we have no choice but to make some approximation. Since h_1 and k_1 are independent identically distributed Gaussian distribution $N(0, \sigma_\xi^2)$, it is easy to know that the distribution function of h is a Rayleigh distribution

$$f(h) = \frac{h}{\sigma_\xi^2} \exp\left(-\frac{h^2}{2\sigma_\xi^2}\right).$$

Therefore, h takes a value concentrated on its expectation

$$Eh = \sqrt{\frac{\pi}{2}}\, \sigma_\xi .$$

Let $\Delta h = h - Eh$, we have

$$E(\Delta h)^2 = \frac{4-\pi}{2}\, \sigma_\xi^2.$$

When compared with Eh, Δh is a small, so we can use the perturbation method to solve equations (47). When $h = Eh$ and $\Delta h = 0$, equations (47) have the following solution

$$\begin{cases} a_0 = \dfrac{1}{\sqrt{\omega}} \left[\dfrac{\sigma}{3\alpha} \pm \dfrac{1}{3\alpha} \sqrt{\dfrac{(Eh)^2 - 4\omega^2\beta^2}{4\omega^2}} \right]^{1/2} \\ \sigma - 3\alpha\omega a_0^2 = \dfrac{Eh}{2\omega} \sin\theta_0. \end{cases}$$

When $\Delta h \neq 0$, let

$$a = a_0 + a_1, \qquad \theta = \theta_0 + \theta_1,$$

where a_1 and θ_1 are small terms. Substituting the above equations into equations (47) and neglecting the non-linear terms, we obtain the linearized equations

$$\begin{cases} a_1' = -\dfrac{1}{4\omega} a_0\, Eh \sin\theta_0\, \theta_1 + \dfrac{1}{4\omega} a_0 \cos\theta_0\, \Delta h \\ \theta_1' = -6\alpha\omega a_0\, a_1 - \dfrac{1}{2\omega} Eh \cos\theta_0\, \theta_1 - \dfrac{1}{2\omega} \sin\theta_0\, \Delta h. \end{cases}$$

The first and second moments of the solution of the above equations, Ea_1 and Ea_1^2, can be obtained by the moment method [1]. For steady state response, one obtains

$$\frac{\mathrm{d}Ea_1}{\mathrm{d}t} = \frac{\mathrm{d}E\theta_1}{\mathrm{d}t} = \frac{\mathrm{d}Ea_1\,\Delta h}{\mathrm{d}t} = \frac{\mathrm{d}E\theta_1\,\Delta h}{\mathrm{d}t} = \frac{\mathrm{d}Ea_1^2}{\mathrm{d}t} = \frac{\mathrm{d}E\theta_1^2}{\mathrm{d}t} = \frac{\mathrm{d}Ea_1\,\theta_1}{\mathrm{d}t} = 0,$$

which yields

$$\frac{1}{4\omega} a_0\, Eh \sin\theta_0\, E\theta_1 = \frac{1}{4\omega} a_0 \cos\theta_0\, E\Delta h$$

$$6\alpha\omega a_0\, Ea_1 + \frac{1}{2\omega} Eh \cos\theta_0\, E\theta_1 = -\frac{1}{2\omega} \sin\theta_0\, E\Delta h$$

$$\frac{1}{4\omega} a_0\, Eh \sin\theta_0\, E(\Delta h\theta_1) = \frac{1}{4\omega} a_0 \cos\theta_0\, E(\Delta h)^2$$

$$6\alpha\omega a_0\, E(a_1\,\Delta h) + \frac{1}{2\omega} \cos\theta_0\, E(\theta_1\,\Delta h) = -\frac{1}{2\omega} \sin\theta_0\, E(\Delta h)^2$$

$$\frac{1}{4\omega} a_0\, Eh \sin\theta_0\, E(a_1\,\theta_1) = \frac{1}{4\omega} a_0 \cos\theta_0\, E(a_1\,\Delta h)$$

$$6\alpha\omega a_0\, E(a_1\,\theta_1) + \frac{1}{2\omega} Eh \cos\theta_0\, E\theta_1^2 = -\frac{1}{2\omega} \sin\theta_0\, E(\Delta h\theta_1)$$

$$-\frac{1}{4\omega} a_0\, Eh \sin\theta_0\, E\theta_1^2 + \frac{1}{4\omega} a_0 \cos\theta_0\, E(\Delta h\theta_1) - 6\alpha\omega a_0\, Ea_1^2$$

$$- \frac{1}{2\omega} Eh \cos\theta_0\, E(\theta_1\, a_1) - \frac{1}{2\omega} \sin\theta_0\, E(a_1\,\Delta h) = 0.$$

The above equations have the solution

$$\left\{ \begin{aligned} E(\theta_1\,\Delta h) &= \frac{1}{Eh} \operatorname{cotan}\theta_0\, E(\Delta h)^2 \\ E(a_1\,\Delta h) &= -\frac{1}{12\alpha\omega a_0^2 \sin\theta_0} E(\Delta h)^2 \\ E(a_1\,\theta_1) &= \frac{1}{Eh} \operatorname{cotan}\theta_0\, E(a_1\,\Delta h) \\ E\theta_1^2 &= \frac{\operatorname{cotan}^2\theta_0}{(Eh)^2} E(\Delta h)^2 \\ Ea_1^2 &= \frac{1}{(12\alpha\omega a_0^2 \sin\theta_0)^2} E(\Delta h)^2. \end{aligned} \right. \tag{48}$$

4.3. NUMERICAL SIMULATION

From section 3.3, ω_k's are distributed uniformly in

$$\left(\Omega_1 - \frac{\gamma}{2}, \Omega_1 + \frac{\gamma}{2}\right).$$

So ω_k can be written as

$$\omega_k = \Omega_1 + \gamma\bar{\omega}_k.$$

From equation (34),

$$\xi(t) = \sqrt{\frac{2\sigma_\xi^2}{N}} \sum_{k=1}^{N} \cos\left[(\Omega_1 + \gamma\bar{\omega}_k)t + \varphi_k\right]$$

$$= \sqrt{\frac{2\sigma_\xi^2}{N}} \sum_{k=1}^{N} \left[\cos(\Omega_1\, t)\cos\left(\frac{\gamma}{\varepsilon}\bar{\omega}_k\, T_1 + \varphi_k\right) - \sin(\Omega_1\, t)\sin\left(\frac{\gamma}{\varepsilon}\bar{\omega}_k\, T_1 + \varphi_k\right)\right].$$

From equation (2), h_1 and k_1 are given by

$$\begin{cases} h_1(T_1) = \sqrt{\dfrac{2\sigma_\xi^2}{N}} \displaystyle\sum_{k=1}^{N} \cos\left(\frac{\gamma}{\varepsilon}\bar{\omega}_k\, T_1 + \varphi_k\right) \\ k_1(T_1) = -\sqrt{\dfrac{2\sigma_\xi^2}{N}} \displaystyle\sum_{k=1}^{N} \sin\left(\frac{\gamma}{\varepsilon}\bar{\omega}_k\, T_1 + \varphi_k\right), \end{cases} \tag{49}$$

where φ_k's are independent and uniformly distributed in $(0, 2\pi)$, $\bar{\omega}_k$'s are independent and uniformly distributed in $(-0{\cdot}5, 0{\cdot}5)$. The time history of h_1 is shown in Figure 11.

Equations (44) are numerically integrated by the fourth order Runge–Kutta algorithm, and equation (45) is numerically integrated by the Simpson algorithm. In the numerical simulation, the parameters in systems (1) and (49) are chosen as follows: $N = 500$, $\gamma = 0{\cdot}1$, $\varepsilon = 0{\cdot}1$, $\beta = 0{\cdot}5$, $\alpha = 0{\cdot}1$, $\omega = 1{\cdot}0$.

The variation of the largest Lyapunov λ governed by equation (45) with σ and σ_ξ^2 is shown in Figure 12 as $\lambda - (\sigma, \sigma_\xi^2)$ surface. When $\lambda = 0$ the corresponding σ_ξ^2–σ curve is

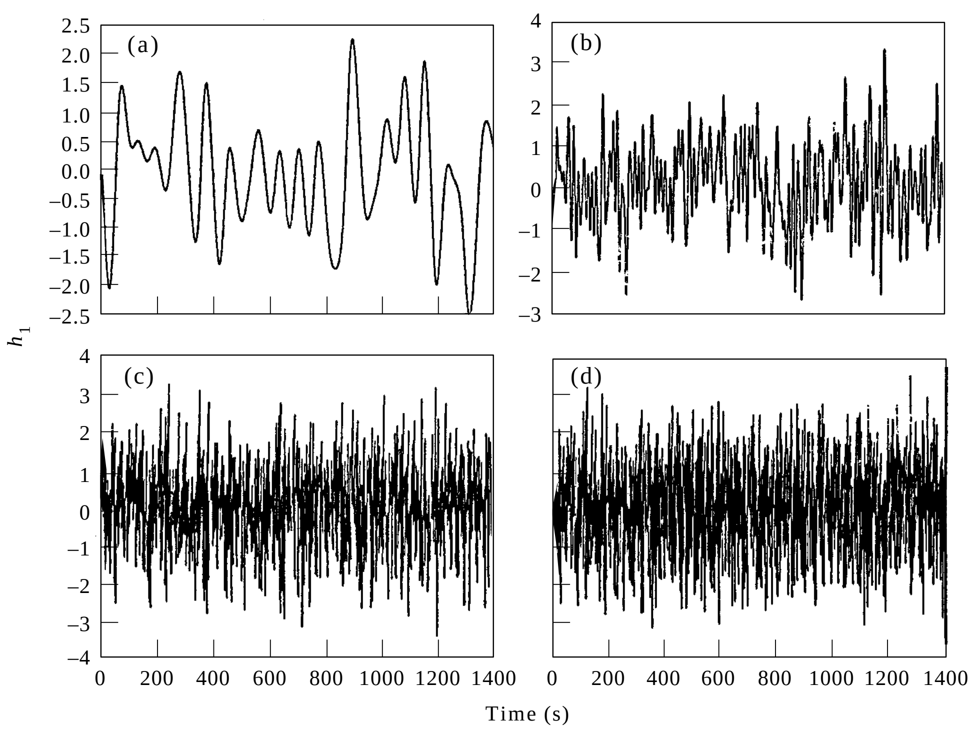

Figure 11. Time history of h_1. (a) $\gamma = 0{\cdot}02$; (b) $\gamma = 0{\cdot}1$; (c) $\gamma = 0{\cdot}5$; (d) $\gamma = 1{\cdot}0$.

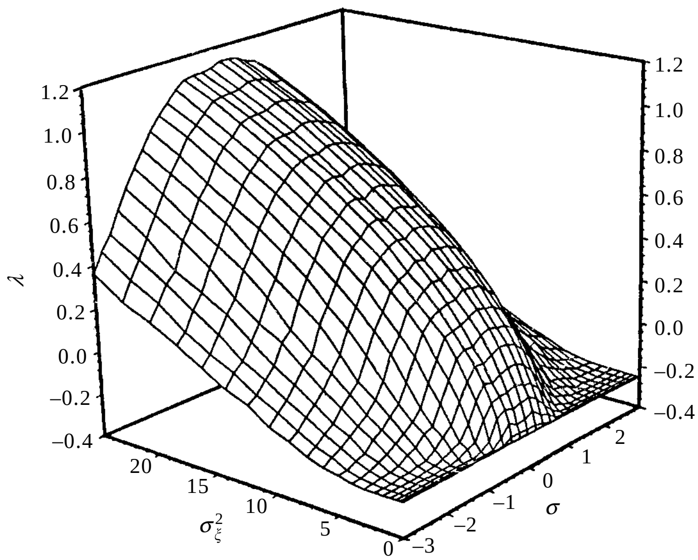

Figure 12. Largest Lyapunov exponent of Duffing system.

shown in Figure 13, which is the almost certain stability boundary of the trivial steady state solution of equations (41). When (σ, σ_ξ^2) is located above the curve, the corresponding trivial steady state solution is not stable; while it is located below the curve, the corresponding trivial steady state solution is stable. The numerical results of the stability boundary of equation (1) by different methods are shown in Figure 14.

As the random excitation σ_ξ^2 becomes larger, equation (1) will have a non-trivial steady state solution. When $\sigma_\xi^2 = 100$, the first and second steady state moments governed by equations (48) are shown in Figure 15 while σ changes from -2 to 2. For comparison in Figure 15, the numerical result of equation (1) is also shown. When $\sigma = 1{\cdot}0$ the variations of Ea and Ea^2 with σ_ξ^2 are shown in Figure 16. When $\sigma = -1$, $h_0 = k_0 = 2$ and

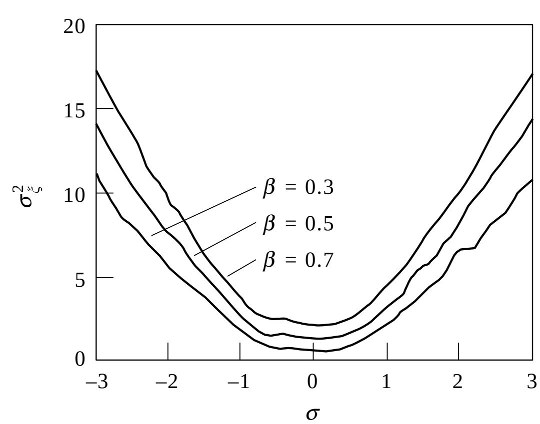

Figure 13. Stability area of Duffing system.

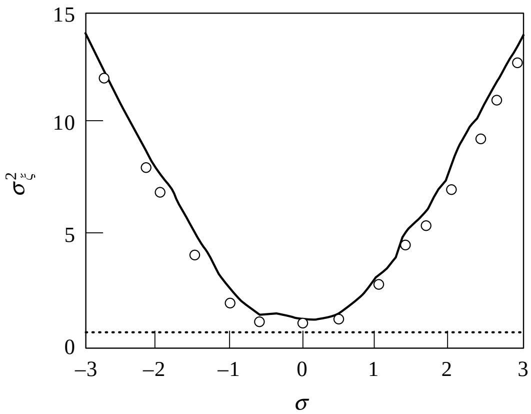

Figure 14. Stability area of Duffing system. ——, Stability area via equation (45); · · · ·, stability area via equation (40); ○○○, stability area via simulation.

$\Omega_0 = 10$, the time histories of $u(t)$ governed by equation (1) for several different values of σ_ξ^2 are shown in Figure 17.

5. PRINCIPAL PARAMETRIC RESONANCE III

Here, the case of principal parametric resonance is considered when $\Omega_0 = \Omega_1 \approx 2\omega$. Introducing the detuning parameter σ as follows

$$\Omega_0 = \Omega_1 = 2\omega + \varepsilon\sigma, \tag{50}$$

one has

$$(\Omega_0 - \omega)T_0 = (\Omega_1 - \omega)T_0 = \omega T_0 + \sigma T_1.$$

By the above assumption, eliminating the secular terms in equation (11) yields

$$2i\omega A' + i\beta\omega A + 3\alpha\omega^2 A^2 \bar{A} + \tfrac{1}{2}\bar{A}[h_0 + h_1 - i(k_0 + k_1)]\exp(i\sigma T_1) = 0. \tag{51}$$

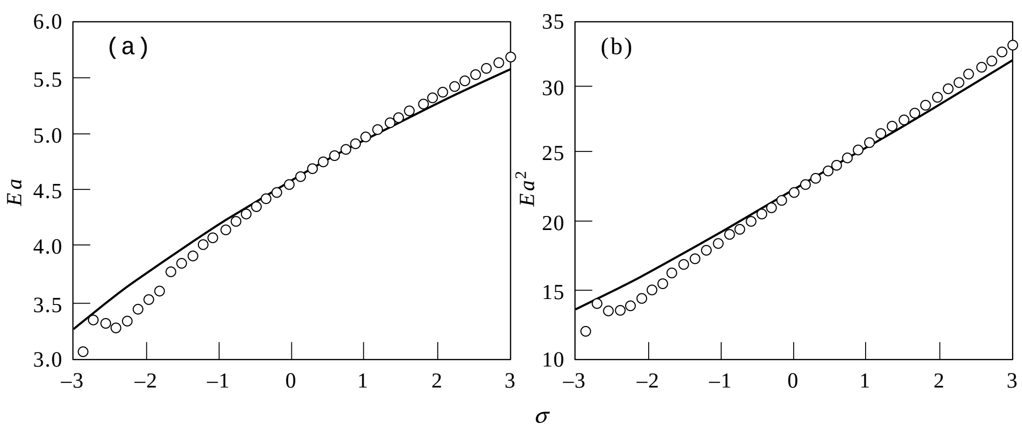

Figure 15. Frequency response of Duffing system: $h_0 = k_0 = 2{\cdot}0$, $\Omega_0 = 10{\cdot}0$, $\sigma_\xi^2 = 100{\cdot}0$. (a) Ea; (b) Ea^2: ——, theoretical solution; ○○○, numerical solution.

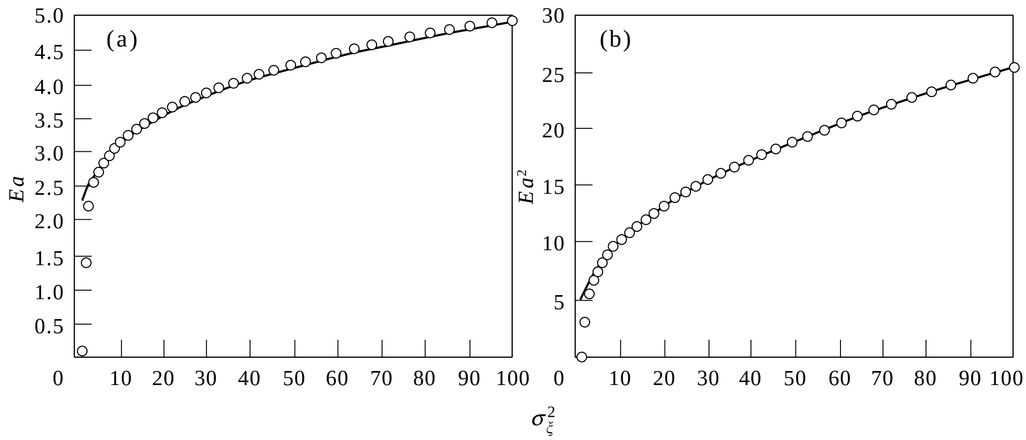

Figure 16. Steady state response of Duffing system: $h_0 = k_0 = 2{\cdot}0$, $\Omega_0 = 10{\cdot}0$, $\sigma = 1{\cdot}0$. (a) Ea; (b) Ea^2: ——, theoretical solution; ○○○, numerical solution.

5.1. TRIVIAL STEADY STATE RESPONSE

Substituting equation (22) into equation (51) and separating the real and imaginary parts of equation (51), one obtains

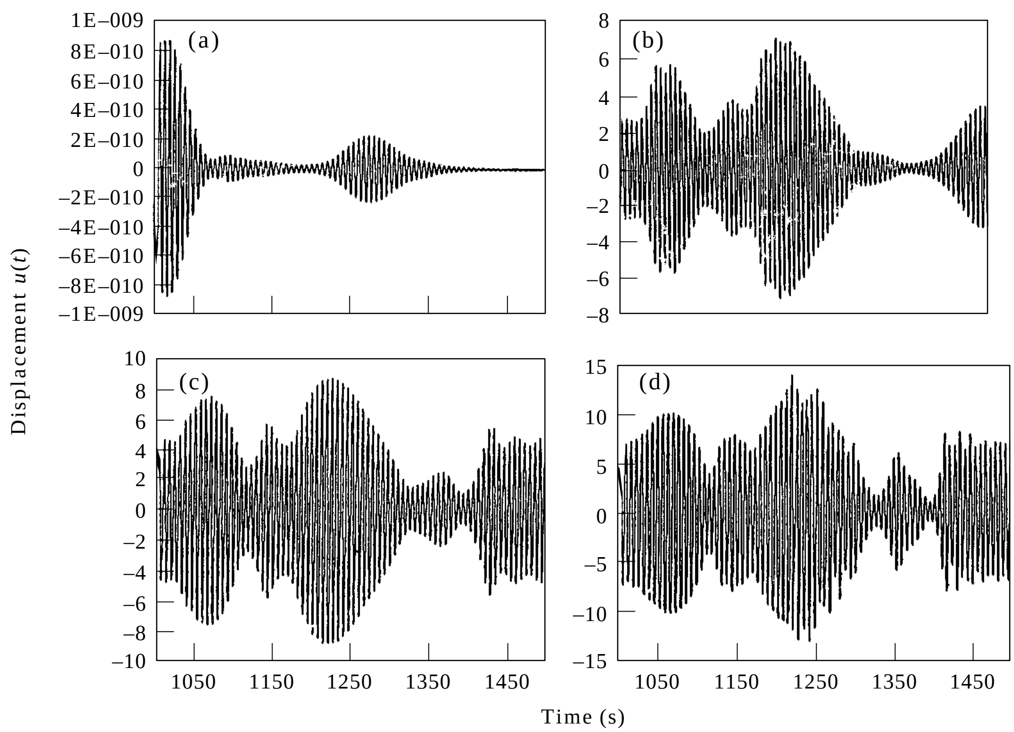

Figure 17. Frequency response of Duffing system: $h_0 = k_0 = 2{\cdot}0$, $\Omega_0 = 10{\cdot}0$. (a) $\sigma_\xi^2 = 1{\cdot}0$; (b) $\sigma_\xi^2 = 9{\cdot}0$; (c) $\sigma_\xi^2 = 25{\cdot}0$; (d) $\sigma_\xi^2 = 100{\cdot}0$.

$$\begin{cases} x' = \left(-\dfrac{\beta}{2} + \dfrac{k_0 + k_1}{4\omega}\right)x + \left(\dfrac{\sigma}{2} + \dfrac{h_0 + h_1}{4\omega}\right)y - \frac{3}{2}\,\alpha\omega(x^2 + y^2)y \\ y' = \left(-\dfrac{\sigma}{2} + \dfrac{h_0 + h_1}{4\omega}\right)x + \left(-\dfrac{\beta}{2} - \dfrac{k_0 + k_1}{4\omega}\right)y + \frac{3}{2}\,\alpha\omega(x^2 + y^2)x. \end{cases} \tag{52}$$

Using a similar technique as shown in section 4.1, we obtain the sufficient almost certain stability condition of the trivial steady state solution of equations (52) as follows

$$\sigma_\xi^2 < \tfrac{1}{4}\,(2\omega\beta - \sqrt{h_0^2 + k_0^2})^2, \qquad \sqrt{h_0^2 + k_0^2} < 2\omega\beta. \tag{53}$$

To obtain the necessary and sufficient almost certain stability condition of equations (52), its linearized equation is considered in the neighborhood of (0, 0)

$$\begin{cases} x' = \left(-\dfrac{\beta}{2} + \dfrac{k_0 + k_1}{4\omega}\right)x + \left(\dfrac{\sigma}{2} + \dfrac{h_0 + h_1}{4\omega}\right)y \\ y' = \left(-\dfrac{\sigma}{2} + \dfrac{h_0 + h_1}{4\omega}\right)x + \left(-\dfrac{\beta}{2} - \dfrac{k_0 + k_1}{4\omega}\right)y. \end{cases} \tag{54}$$

Substituting equations (43) into equations (54), one obtains

$$\begin{cases} a' = -\dfrac{\beta}{2}\,a + \dfrac{a}{4\omega}\,[(k_0 + k_1)\cos\eta - (h_0 + h_1)\sin\eta] \\ \eta' = \sigma - \dfrac{1}{2\omega}\,[(h_0 + h_1)\cos\eta + (k_0 + k_1)\sin\eta] \\ \rho' = -\dfrac{\beta}{2} + \dfrac{1}{4\omega}\,[(k_0 + k_1)\cos\eta - (h_0 + h_1)\sin\eta]. \end{cases} \tag{55}$$

Then the largest Lyapunov exponent of the trivial steady state solution of equations (54) may be found as

$$\lambda = -\frac{\beta}{2} + \frac{1}{4\omega}\lim_{T\to\infty}\frac{1}{T}\int_0^T [(k_0 + k_1)\cos\eta(T_1) - (h_0 + h_1)\sin\eta(T_1)]\,\mathrm{d}T_1. \tag{56}$$

When $\lambda < 0$ the trivial solution is stable, when $\lambda > 0$ the trivial solution is unstable.

5.2. NON-TRIVIAL STEADY STATE RESPONSE

For small σ_ξ^2, when the parameters $(\sigma, \sqrt{h_0^2 + k_0^2})$ of equation (51) are located in area I or III, equation (51) has only a trivial steady state response. As σ_ξ^2 gets larger, the trivial steady state solution will become unstable. When the parameters $(\sigma, \sqrt{h_0^2 + k_0^2})$ of equation (51) are located in area II, equation (51) will have a non-trivial steady state solution. To obtain the first and second steady state moments, we use transformation (14) and rewrite equation (51) into

$$\begin{cases} a' = -\dfrac{\beta}{2}\,a + \dfrac{a}{4\omega}\,[(k_0 + k_1)\cos\eta - (h_0 + h_1)\sin\eta] \\ \eta' = \sigma - 3\alpha\omega a^2 - \dfrac{1}{2\omega}\,[(h_0 + h_1)\cos\eta + (k_0 + k_1)\sin\eta]. \end{cases} \tag{57}$$

Then the first order approximate solution of equation (1) takes the same form as shown in equation (16). Hence, by taking temporal average, equations (57) can be reduced to

$$\begin{cases} a' = -\dfrac{\beta}{2} a + \dfrac{a}{4\omega} h \cos\theta \\ \\ \theta' = \sigma - 3\alpha\omega a^2 - \dfrac{h}{2\omega}\sin\theta, \end{cases} \tag{58}$$

where

$$\theta = \arctan\frac{k_0 + k_1}{h_0 + h_1} + \eta, \qquad h = \sqrt{(h_0 + h_1)^2 + (k_0 + k_1)^2}.$$

Here the fast varying terms such as $(h_0 + h_1)W_2$ and $(k_0 + k_1)W_2$, and the small terms such as $\gamma k_1(h_0 + h_1)$ and $\gamma h_1(k_0 + k_1)$, i.e., $(\arctan(k_0 + k_1)/(h_0 + h_1))'$ are set to zero in the reduction of equations (57) to (58). Equations (58) have the same form as equations (47), and so the discussions in section 4.2 are also available here, except Eh and $E(\Delta h)^2$ in equations (48) should be changed to

$$\begin{cases} Eh = E\sqrt{(h_0 + h_1)^2 + (k_0 + k_1)^2} \\ \quad = \dfrac{1}{2\pi\sigma_\xi^2}\displaystyle\int_{-\infty}^{+\infty}\int_{-\infty}^{+\infty}\sqrt{(h_0 + x)^2 + (k_0 + y)^2}\exp\left(-\frac{x^2 + y^2}{2\sigma_\xi^2}\right)\mathrm{d}x\,\mathrm{d}y \\ E(\Delta h)^2 = 2\sigma_\xi^2 - (Eh)^2 + h_0^2 + k_0^2. \end{cases} \tag{59}$$

From equations (48) the first and second steady state moments Ea and Ea^2 of equation (51) can be obtained.

When the parameters $(\sigma, \sqrt{h_0^2 + k_0^2})$ are located in area II or III and $\sigma_\xi^2 = 0$, the steady state response of equation (51) corresponds to (a_0, η_0), which satisfies equations (17). When the random excitations σ_ξ^2 are small, the first and second steady state solution of equations (57) can be obtained by perturbation method by assuming

$$a = a_0 + a_1, \qquad \eta = \eta_0 + \eta_1, \tag{60}$$

where a_1 and η_1 are small terms. Substituting equations (60) into equations (57) and neglecting the non-linear terms, we obtain the linearized equation

$$\begin{cases} a_1' = \dfrac{1}{4\omega}(k_1\cos\eta_0 - h_1\sin\eta_0)a_1 - \dfrac{a_0}{4\omega}[(k_0 + k_1)\sin\eta_0 + (h_0 + h_1)\cos\eta_0]\eta_1 \\ \qquad + \dfrac{a_0}{4\omega}(k_1\cos\eta_0 - h_1\sin\eta_0) \\ \eta_1' = -6\alpha\omega a_0 a_1 + \left[-\beta + \dfrac{1}{2\omega}(-k_1\cos\eta_0 + h_1\sin\eta_0)\right]\eta_1 \\ \qquad - \dfrac{1}{2\omega}(h_1\cos\eta_0 + k_1\sin\eta_0). \end{cases} \tag{61}$$

where h_1 and k_1 are governed by equations (5). Ea and Ea^2 can be obtained by moment method. For the steady state moments, one has

$$\mathrm{u}\frac{\mathrm{d}Ea_1}{\mathrm{d}t} = \frac{\mathrm{d}E\eta_1}{\mathrm{d}t} = \frac{\mathrm{d}Ea_1\,h_1}{\mathrm{d}t} = \frac{\mathrm{d}Ea_1\,k_1}{\mathrm{d}t}$$

$$= \frac{\mathrm{d}E\eta_1\,h_1}{\mathrm{d}t} = \frac{\mathrm{d}E\eta_1\,k_1}{\mathrm{d}t} = \frac{\mathrm{d}Ea_1^2}{\mathrm{d}t} = \frac{\mathrm{d}E\eta_1^2}{\mathrm{d}t} = 0,$$

with $Eh_1^2 = Ek_1^2 = \sigma_\xi^2$. The above equations yield

$$\frac{1}{4\omega}(\cos\eta_0\,Ea_1\,k_1 - \sin\eta_0\,Ea_1\,h_1) - \frac{a_0}{4\omega}(k_0\sin\eta_0 + h_0\cos\eta_0)E\eta_1$$

$$- \frac{a_0}{4\omega}(\sin\eta_0\,E\eta_1\,k_1 + \cos\eta_0\,E\eta_1\,h_1) = 0$$

$$-6\alpha\omega a_0\,Ea_1 - \beta E\eta_1 + \frac{1}{2\omega}(\sin\eta_0\,E\eta_1\,h_1 - \cos\eta_0\,E\eta_1\,k_1) = 0$$

$$\frac{\bar{\gamma}}{2}Ea_1\,h_1 + \frac{a_0}{4\omega}(k_0\sin\eta_0 + h_0\cos\eta_0)E\eta_1\,h_1 = -\frac{a_0}{4\omega}\sin\eta_0\,\sigma_\xi^2$$

$$\frac{\bar{\gamma}}{2}Ea_1\,k_1 + \frac{a_0}{4\omega}(k_0\sin\eta_0 + h_0\cos\eta_0)E\eta_1\,k_1 = \frac{a_0}{4\omega}\cos\eta_0\,\sigma_\xi^2$$

$$6\alpha\omega a_0\,Ea_1\,h_1 + \left(\beta + \frac{\bar{\gamma}}{2}\right)E\eta_1\,h_1 = -\frac{1}{2\omega}\cos\eta_0\,\sigma_\xi^2$$

$$6\alpha\omega a_0\,Ea_1\,k_1 + \left(\beta + \frac{\bar{\gamma}}{2}\right)E\eta_1\,k_1 = -\frac{1}{2\omega}\sin\eta_0\,\sigma_\xi^2$$

$$(k_0\sin\eta_0 + h_0\cos\eta_0)Ea_1\,\eta_1 = \cos\eta_0\,Ea_1\,k_1 - \sin\eta_0\,Ea_1\,h_1$$

$$E\eta_1^2 = -\frac{1}{2\beta}\left[12\alpha\omega a_0\,E\eta_1\,a_1 + \frac{1}{\omega}(\cos\eta_0\,E\eta_1\,h_1 + \sin\eta_0 E\eta_1\,k_1)\right]$$

$$Ea_1^2 = \frac{1}{6\alpha\omega a_0}\left[-\frac{a_0}{4\omega}(k_0\sin\eta_0 + h_0\cos\eta_0)E\eta_1^2 - \beta Ea_1\,\eta_1\right.$$

$$\left. - \frac{1}{2\omega}(\cos\eta_0\,Ea_1\,h_1 + \sin\eta_0\,Ea_1\,k_1) + \frac{a_0}{4\omega}(\cos\eta_0\,E\eta_1\,k_1 - \sin\eta_0\,E\eta_1\,h_1)\right],$$

where $\bar{\gamma} = \gamma/\varepsilon$. The solutions of the above equations are

$$\left\{\begin{aligned} Ea_1 h_1 &= \left[\frac{1}{\omega}\Delta_1 \cos\eta_0 - (2\beta + \bar{\gamma})\sin\eta_0\right]\frac{a_0}{2\Delta_2\,\omega}\sigma_\xi^2 \\ Ea_1 k_1 &= \left[\frac{1}{\omega}\Delta_1 \sin\eta_0 + (2\beta + \bar{\gamma})\cos\eta_0\right]\frac{a_0}{2\Delta_2\,\omega}\sigma_\xi^2 \\ E\eta_1 h_1 &= (6\alpha\omega a_0^2 \sin\eta_0 - \bar{\gamma}\cos\eta_0)\frac{1}{\Delta_2\,\omega}\sigma_\xi^2 \\ E\eta_1 k_1 &= -(6\alpha\omega a_0^2 \cos\eta_0 + \bar{\gamma}\sin\eta_0)\frac{1}{\Delta_2\,\omega}\sigma_\xi^2 \\ Ea_1\eta_1 &= \frac{2\beta+\bar{\gamma}}{\Delta_1}\frac{a_0}{2\Delta_2\,\omega}\sigma_\xi^2 \\ E\eta_1 &= \frac{2\beta+3\bar{\gamma}}{\Delta_1}\frac{1}{2\Delta_2\,\omega}\sigma_\xi^2 \\ Ea_1 &= \frac{1}{6\alpha\omega a_0}\left[-\frac{\beta(2\beta+3\bar{\gamma})}{\Delta_1} + 6\alpha a_0^2\right]\frac{1}{2\Delta_2\,\omega}\sigma_\xi^2, \end{aligned}\right. \tag{62}$$

where

$$\Delta_1 = k_0 \sin\eta_0 + h_0 \cos\eta, \qquad \Delta_2 = (2\beta + \bar{\gamma})\bar{\gamma} - 6\alpha a_0^2 k_0\,\Delta_1.$$

Since (a_0, η_0) satisfies equations (17) and $\Delta_1 < 0$, from equations (62) we can conclude that $Ea_1 > 0$, i.e., the random excitation changes the response of the system from a limit cycle to a diffused limit cycle and the radius of the cycle will become large when σ_ξ^2 increases.

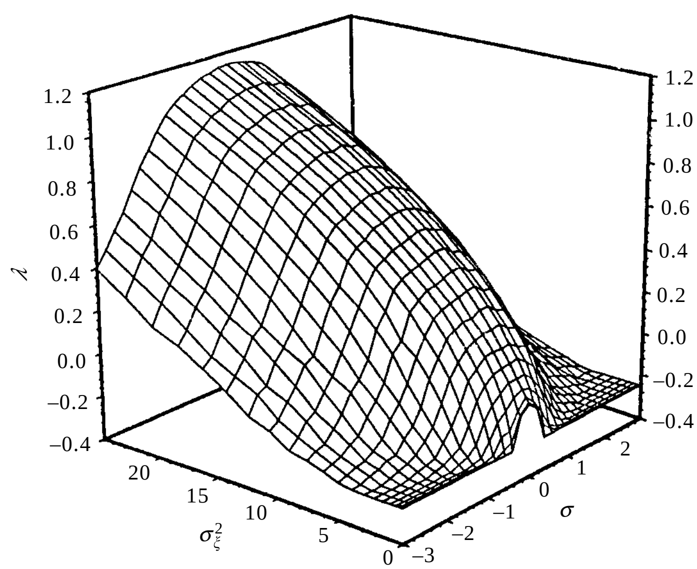

Figure 18. Largest Lyapunov exponent of Duffing system: $h_0 = k_0 = 0{\cdot}5$, $\Omega_0 = \Omega_1$.

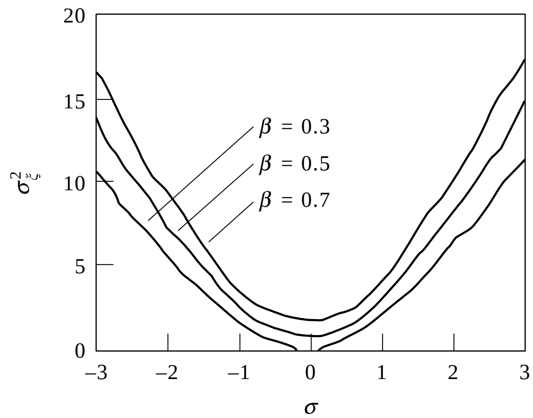

Figure 19. Stability area of Duffing system: $h_0 = k_0 = 0{\cdot}5$, $\Omega_0 = \Omega_1$.

By a similar technique as used in section 5.1, the largest Lyapunov exponent of the solutions a_1 and η_1 can be obtained as

$$\begin{cases} \varphi' = (c_3 - c_2) + (c_2 + c_3)\cos\varphi + (c_4 - c_1)\sin\varphi \\ \lambda = -\dfrac{\beta}{2} + \tfrac{1}{2}\lim\limits_{T\to\infty}\dfrac{1}{T}\displaystyle\int_0^T [(c_1 - c_4)\cos\varphi(T_1) + (c_2 + c_3)\sin\varphi(T_1)]\,\mathrm{d}T_1, \end{cases} \tag{63}$$

where

$$c_1 = \frac{1}{4\omega}(k_1\cos\eta_0 - h_1\sin\eta_0),$$

$$c_2 = -\frac{a_0}{4\omega}[(k_0 + k_1)\sin\eta_0 + (h_0 + h_1)\cos\eta_c],$$

$$c_3 = -6\alpha\omega a_0,$$

$$c_4 = -\beta + \frac{1}{2\omega}(h_1\sin\eta_0 - k_1\cos\eta_0).$$

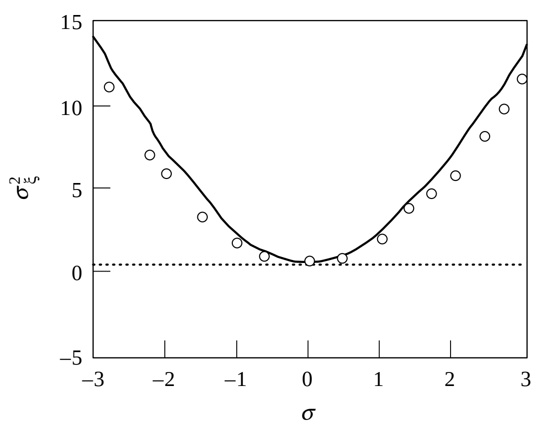

Figure 20. Stability area of Duffing system: $h_0 = k_0 = 0{\cdot}5$, $\Omega_0 = \Omega_1$. ——, Stability area via equation (45); · · · · , stability area via equation (40); ○○○, stability area via simulation.

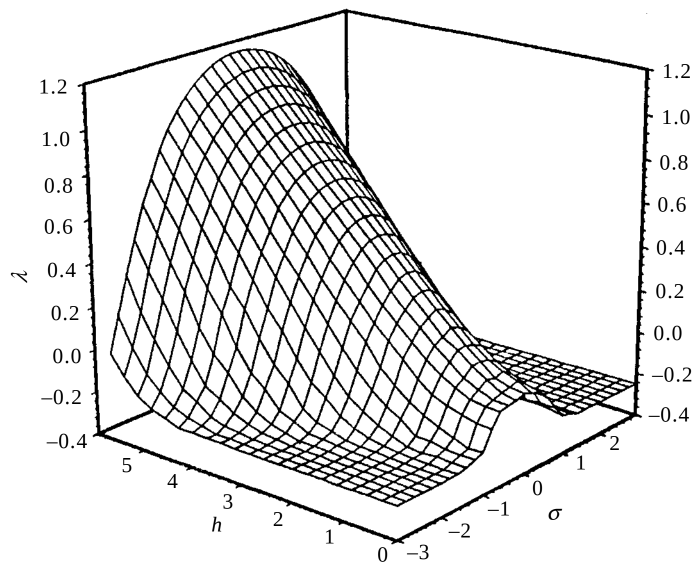

Figure 21. Largest Lyapunov exponent of Duffing system: $\sigma_\xi^2 = 1{\cdot}0$, $\Omega_0 = \Omega_1$.

5.3. NUMERICAL SIMULATION

In the numerical simulation, the parameters in systems (1) and (49) are chosen as follows: $N = 500$, $\gamma = 0{\cdot}1$, $\varepsilon = 0{\cdot}1$, $\beta = 0{\cdot}5$, $\alpha = 0{\cdot}1$, $\omega = 1{\cdot}0$. When $h_0 = k_0 = 0{\cdot}5$, the variation of the largest Lyapunov λ governed by equation (56) with σ and σ_ξ^2 is shown in Figure 18 as $\lambda - (\sigma, \sigma_\xi^2)$ surface. When $\lambda = 0$ the corresponding σ_ξ^2–σ curves are shown in Figure 19. The numerical results of the stability boundary of equation (1) are shown in Figure 20. Figure 21 shows the variation of the largest Lyapunov exponent λ governed by equation (56) with σ and $h = \sqrt{h_0^2 + k_0^2}$, when $\sigma_\xi^2 = 1{\cdot}0$. When $\lambda = 0$, the corresponding stability boundaries are shown in Figure 22. When $\sigma_\xi^2 = 100$, the theoretical solutions governed by equations (59) and (48), and the numerical results of equation (1) are shown in Figure 23. When $h_0 = k_0 = 2$, the theoretical and numerical results are shown in Figure 24. When $\sigma_\xi^2 = 0{\cdot}1$, $h_0 = k_0 = 2$, the theoretical solution governed by equations (62) is compared with the numerical result of equation (1) in Figure 25. When $h_0 = k_0 = 2$, the variation of the largest Lyapunov exponent λ of equations (63) is shown in Figure 26 as $\lambda - (\sigma, \sigma_\xi^2)$

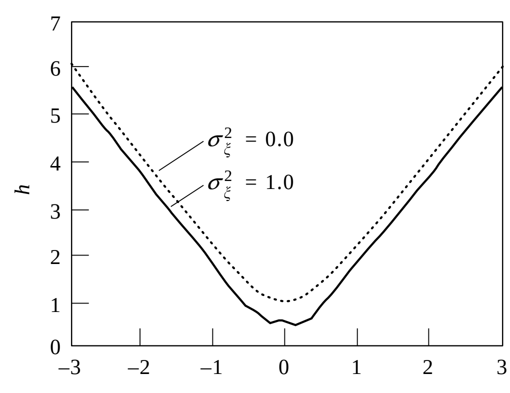

Figure 22. Stability area of Duffing system ($\Omega_0 = \Omega_1$).

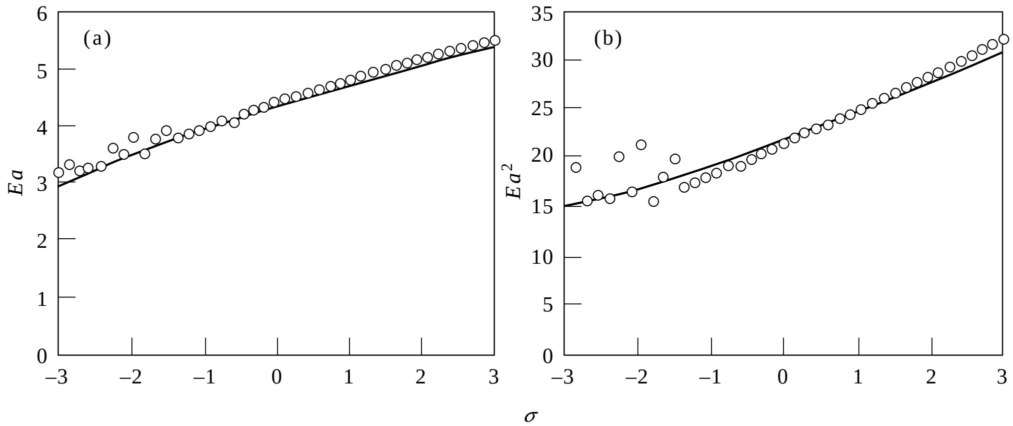

Figure 23. Frequency response of Duffing system: $h_0 = k_0 = 2{\cdot}0$, $\Omega_0 = \Omega_1$, $\sigma_\xi^2 = 100{\cdot}0$. (a) Ea; (b) Ea^2: ——, theoretical solution; ○○○, numerical solution.

surfaces. When $\lambda = 0$, the corresponding σ_ξ^2–σ curve is shown in Figure 27. In Figures 28–30, the numerical results of equation (1) are shown when $\sigma = 1$, $h_0 = k_0 = 2$, and it can be seen that the responses of equation (1) are diffused limit cycles when σ_ξ^2 increases.

5.4. BIFURCATION AND JUMPS

While considering the almost certain stability bifurcation, the largest Lyapunov exponent λ can be treated as a bifurcation indicator. When $\lambda < 0$ the solution is stable and when $\lambda > 0$ the solution is unstable. If σ_ξ^2 is chosen to be the bifurcation parameter and $h = \sqrt{h_0^2 + k_0^2}$, σ to be constant, when σ_ξ^2 increases from a small value, the trivial solution of equation (51) will become unstable and the bifurcation of the steady state response is shown in Figure 19. If $|\sigma|$ is chosen to be the bifurcation parameter and σ_ξ^2 to be constant, the trivial solution of equation (51) will become unstable and the bifurcation of the steady state response is also shown in Figure 19. If h is chosen to be the bifurcation parameter and σ_ξ^2, σ to be constants, when h increases from a small value to a certain threshold value,

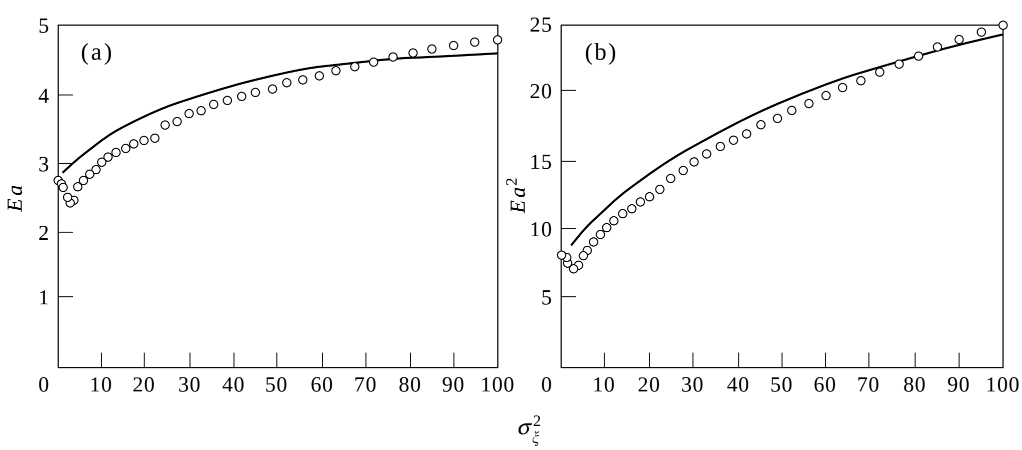

Figure 24. Steady state response of Duffing system: $h_0 = k_0 = 2{\cdot}0$, $\Omega_0 = \Omega_1$, $\sigma = 1{\cdot}0$. (a) Ea; (b) Ea^2: ——, theoretical solution; ○○○, numerical solution.

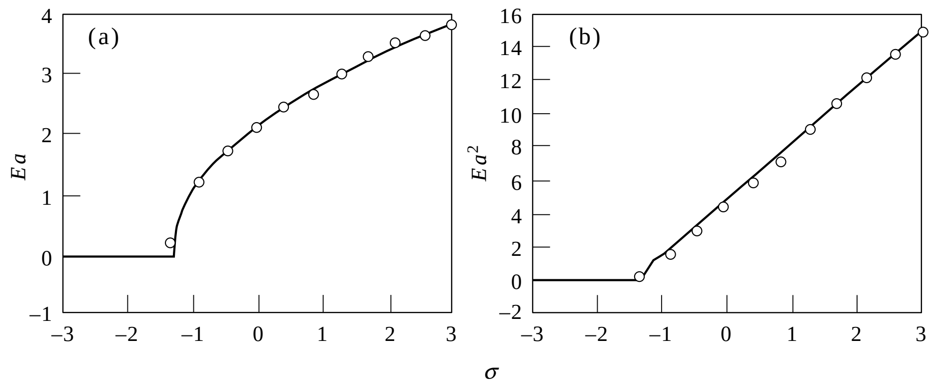

Figure 25. Frequency response of Duffing system: $h_0 = k_0 = 2{\cdot}0$, $\Omega_0 = \Omega_1$, $\sigma_\xi^2 = 0{\cdot}1$. (a) Ea; (b) Ea^2: ——, theoretical solution; ○○○, numerical solution.

the trivial solution of equation (51) will become unstable, and the bifurcation of the steady state response is shown in Figure 22.

When the parameters (σ, h) are located in area III and $\sigma_\xi^2 = 0$, from section 2 it can be seen that equation (51) has two kinds of steady state solutions, i.e., trivial and non-trivial solutions dependent on different initial values. For small σ_ξ^2 these two steady state solutions are stable, which can be observed in the numerical simulation. For small σ_ξ^2 jumps are also observed.

6. PRINCIPAL PARAMETRIC RESONANCE IV

Here, the case of principal parametric resonance is considered when $\Omega_0 \approx 2\omega$, $\Omega_1 \approx 2\omega$, $\Omega_0 \neq \Omega_1$. Introduce the detuning parameters σ and κ as follows

$$\Omega_0 = 2\omega + \varepsilon\sigma, \qquad \Omega_1 = \Omega_0 + \varepsilon\kappa = 2\omega + \varepsilon(\sigma + \kappa).$$

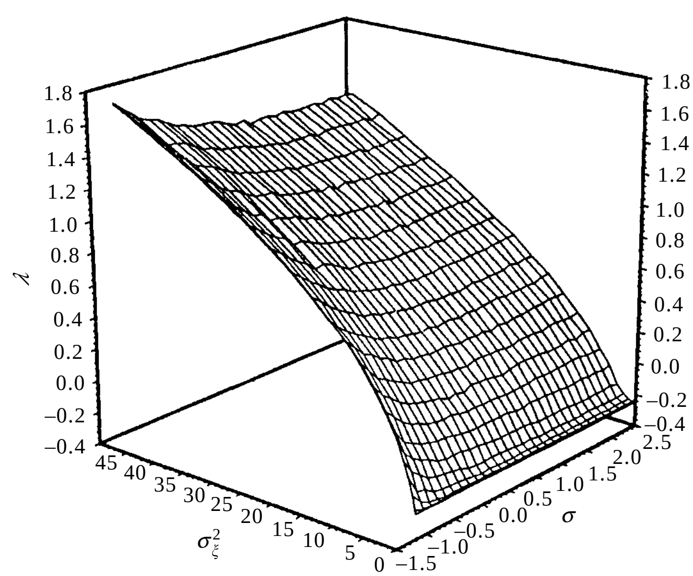

Figure 26. Largest of the perturbation solution: $h_0 = k_0 = 2{\cdot}0$, $\Omega_0 = \Omega_1$.

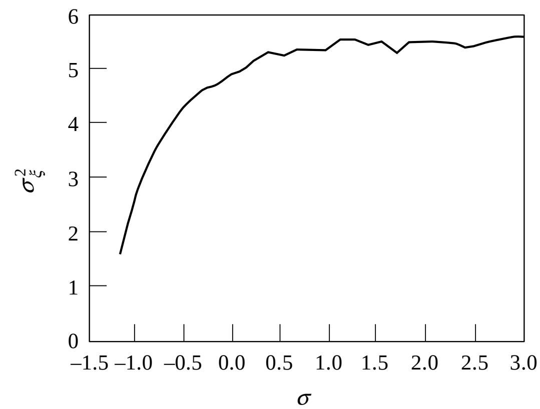

Figure 27. Stability area of the perturbation solution; $h_0 = k_0 = 2{\cdot}0$, $\Omega_0 = \Omega_1$.

After eliminating the secular terms in equation (11), one has

$$2i\omega A' + i\beta\omega A + 3\alpha\omega^2 A^2 \bar{A} + \tfrac{1}{2}\bar{A}(h_c - ik_0)\exp(i\sigma T_1)$$

$$+ \tfrac{1}{2}\bar{A}(h_1 - ik_1)\exp(i(\sigma + \kappa)T_1) = 0. \tag{64}$$

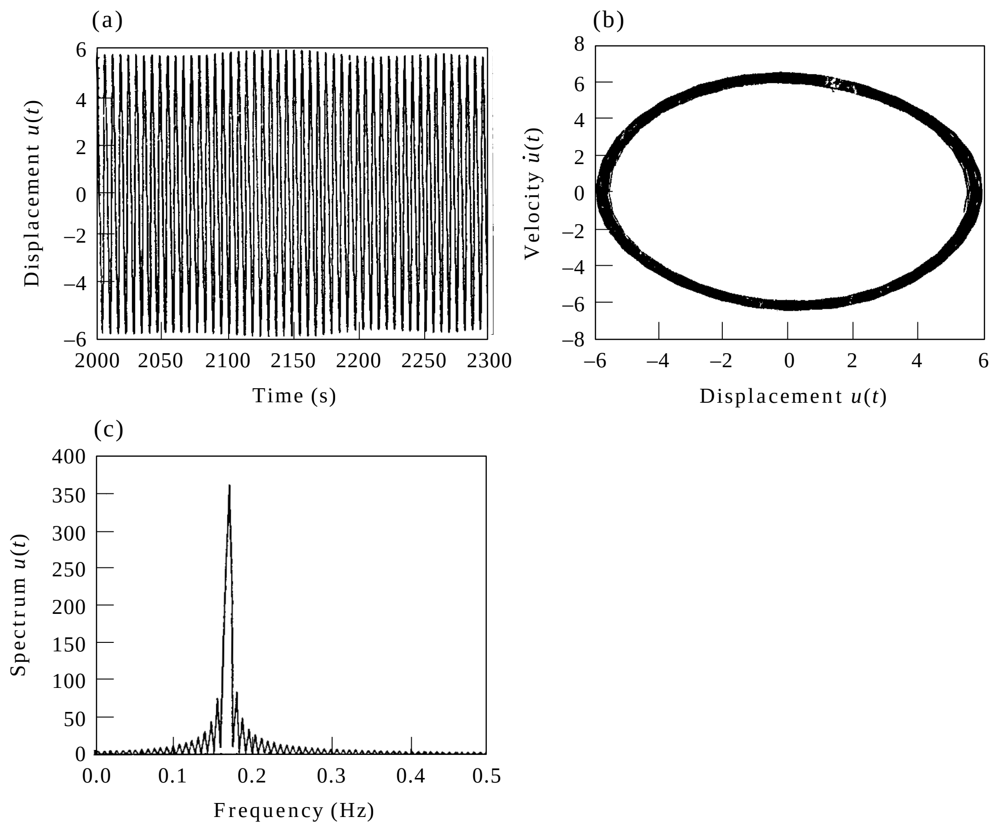

Figure 28. Numerical results of equation (1): $h_0 = k_0 = 2{\cdot}0$, $\Omega_0 = \Omega_1$, $\sigma_\xi^2 = 0{\cdot}1$. (a) Time history of $u(t)$; (b) phase plot; (c) spectrum with frequency of $u(t)$.

Substituting equation (22) into equation (64) yields

$$\begin{cases} x' = \left(-\dfrac{\beta}{2} + \dfrac{k_0}{4\omega}\right)x + \left(\dfrac{\sigma}{2} + \dfrac{h_0}{4\omega}\right)y - \frac{3}{2}\alpha\omega(x^2 + y^2)y \\ \qquad + \dfrac{1}{4\omega}[(xk_1 + yh_1)\cos(\kappa T_1) - (xh_1 - yk_1)\sin(\kappa T_1)] \\ y' = \left(-\dfrac{\sigma}{2} + \dfrac{h_0}{4\omega}\right)x + \left(-\dfrac{\beta}{2} - \dfrac{k_0}{4\omega}\right)y + \frac{3}{2}\alpha\omega(x^2 + y^2)x \\ \qquad + \dfrac{1}{4\omega}[(xh_1 - yk_1)\cos(\kappa T_1) + (xk_1 + yh_1)\sin(\kappa T_1)]. \end{cases} \tag{65}$$

By a similar technique as used in section 4.1 one can obtain the sufficient almost certain stability of the trivial steady state solution of equations (65) as follows

$$\sigma_\xi^2 < \tfrac{1}{16}(2\omega\beta - \sqrt{h_0^2 + k_0^2})^2, \qquad \sqrt{h_0^2 + k_0^2} < 2\omega\beta. \tag{66}$$

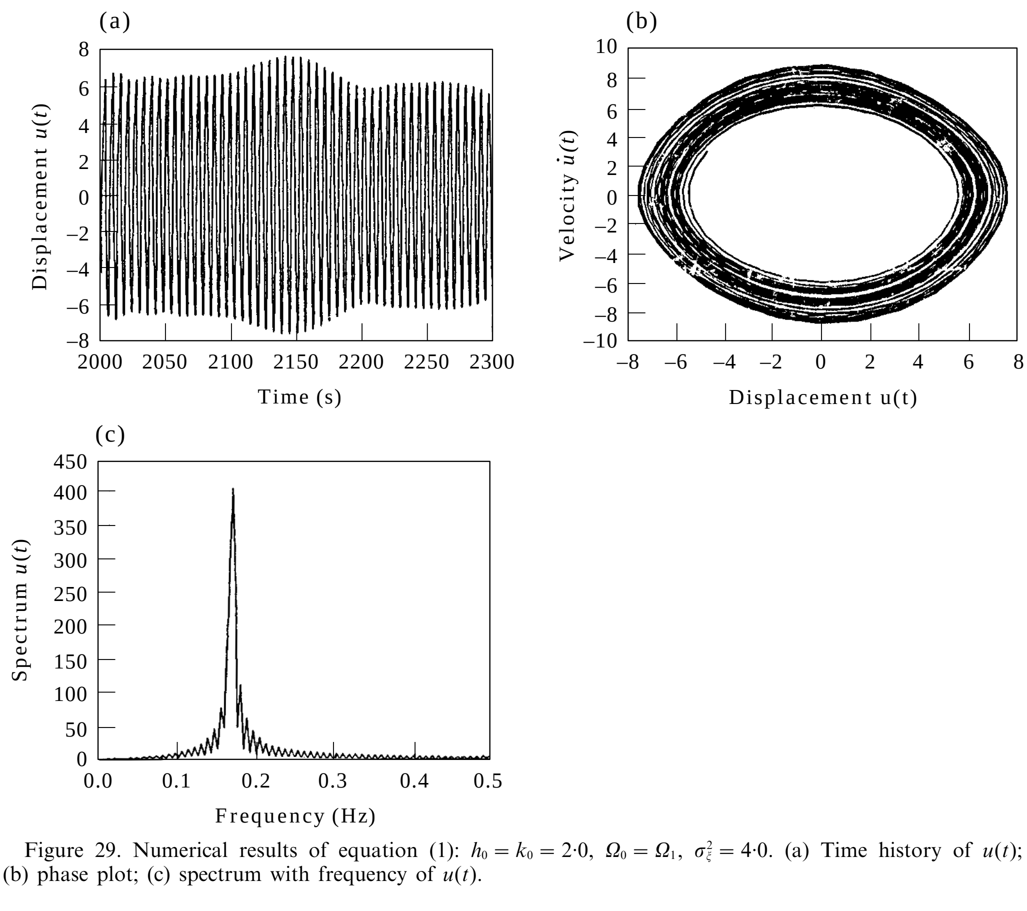

Figure 29. Numerical results of equation (1): $h_0 = k_0 = 2{\cdot}0$, $\Omega_0 = \Omega_1$, $\sigma_\xi^2 = 4{\cdot}0$. (a) Time history of $u(t)$; (b) phase plot; (c) spectrum with frequency of $u(t)$.

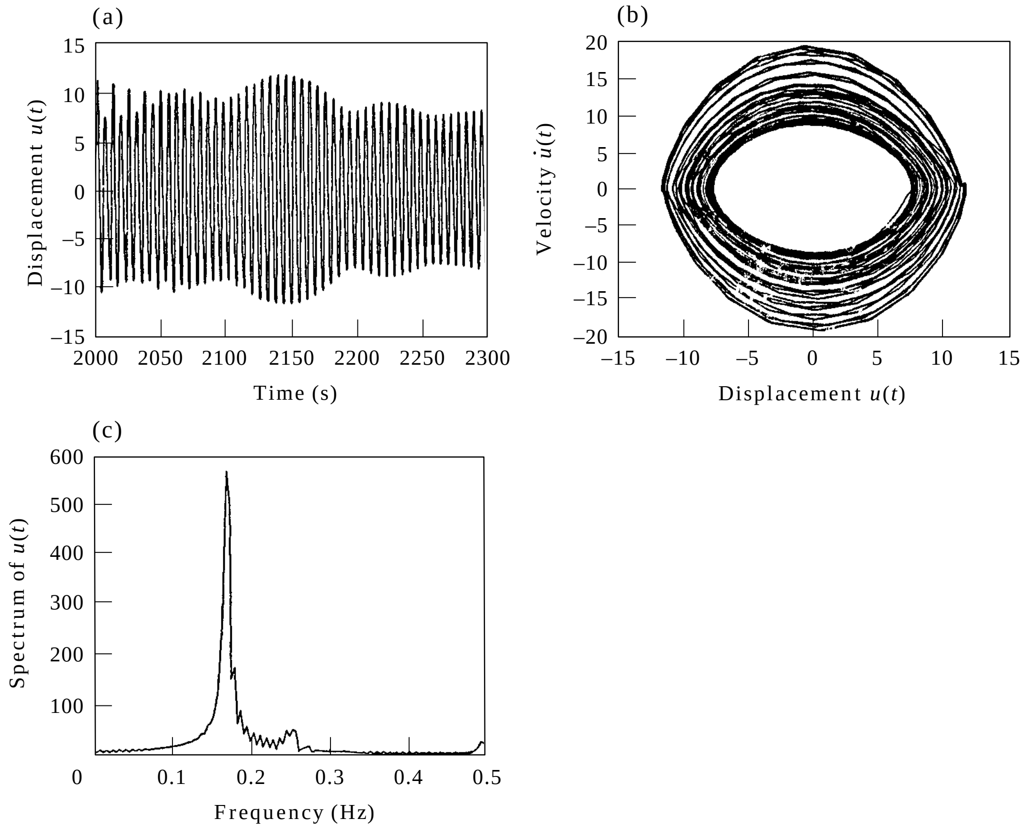

Figure 30. Numerical results of equation (1): $h_0 = k_0 = 2{\cdot}0$, $\Omega_0 = \Omega_1$, $\sigma_\xi^2 = 100{\cdot}0$. (a) Time history of $u(t)$; (b) phase plot; (c) spectrum with frequency of $u(t)$.

Since equations (65) contain the random terms h_1, k_1 and the time-varying terms $\sin \kappa T_1, \cos \kappa T_1$, it is difficult to obtain the sufficient and necessary stability conditions of the trivial solution. For the same reason it is difficult to obtain the steady state moments.

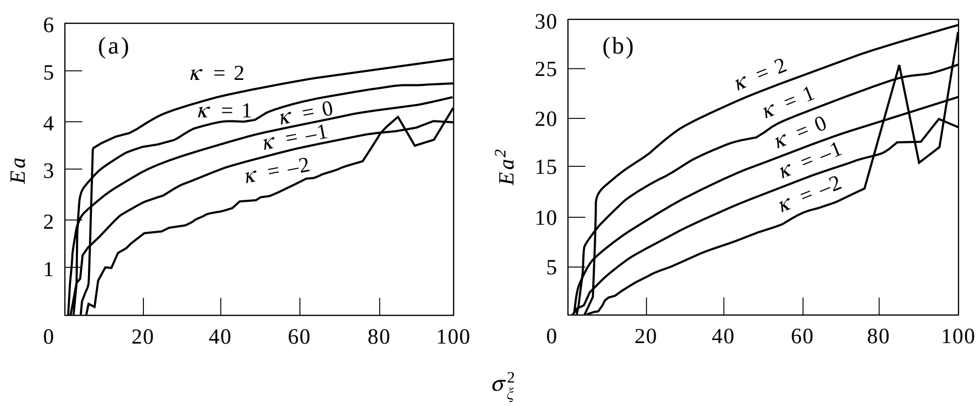

Figure 31. Steady state response of Duffing system: $h_0 = k_0 = 0{\cdot}5$, $\Omega_0 = 2{\cdot}0$. (a) Ea; (b) Ea^2.

Substituting equation (14) into equation (64) yields

$$a' = -\frac{\beta}{2}a + \frac{a}{4\omega}[(k_0\cos\eta - h_0\sin\eta) + k_1\cos(\eta+\kappa T_1) - h_1\sin(\eta+\kappa T_1)]$$

$$\eta' = \sigma - 3\alpha\omega a^2 - \frac{1}{2\omega}[(h_0\cos\eta + k_0\sin\eta) + h_1\cos(\eta+\kappa T_1) + k_1\sin(\eta+\kappa T_1)]. \quad (67)$$

When (σ, h) are located in the parameter area II or III and $\sigma_\xi^2 = 0$, equation (64) has a non-trivial steady state response (a_0, η_0). When σ_ξ^2 is small, the steady state moments governed by equation (64) can be obtained by the perturbation method. Let

$$h_1 = \sigma_\xi \bar{h}_1, \qquad k_1 = \sigma_\xi \bar{k}_1, \qquad a = a_0 + \sigma_\xi a_1 + \cdots, \qquad \eta = \eta_0 + \sigma_\xi \eta_1 + \cdots. \quad (68)$$

Substituting equation (68) into equations (67), and equating coefficient of like power of σ_ξ, one obtains

$$a_1' = \frac{a_0}{4\omega}[-(k_0\sin\eta_0 + h_0\cos\eta_0]\eta_1 + \bar{k}_1\cos(\eta_0+\kappa T_1) - \bar{h}_1\sin(\eta_0+\kappa T_1)]$$

$$\eta_1' = -6\alpha\omega a_0 a_1 - \beta\eta_1 - \frac{1}{2\omega}[\bar{h}_1\cos(\eta_0+\kappa T_1) + \bar{k}_1\sin(\eta_0+\kappa T_1)]. \quad (69)$$

The steady state moments Ea_1, Ea_1^2 can then be obtained by the modal analysis method [9, 13].

Since it is difficult to analyze equation (1) theoretically in this case, the numerical simulation is done here. In the numerical simulation, the parameters in systems (1) and (49) are chosen as follows: $N = 500$, $\gamma = 0{\cdot}1$, $\varepsilon = 0{\cdot}1$, $\beta = 0{\cdot}5$, $\alpha = 0{\cdot}1$, $\omega = 1{\cdot}0$.

It is found that the effects of the random excitation are similar to the case in the principal parametric response III, i.e., when σ_ξ^2 increases, the trivial steady state solution of equation (1) may lose its stability and the non-trivial steady state solution may be changed from a limit cycle to a diffused limit cycle. Under some conditions the system may have two steady state solutions and jumps can be observed. When $h_0 = k_0 = 0{\cdot}5$, $\Omega_0 = 2{\cdot}0$, $\Omega_1 = 2 + 0{\cdot}1\kappa$, the numerical results of the response of equation (1) are shown in Figure 31. When $h_0 = k_0 = 2{\cdot}0$, $\Omega_0 = 2{\cdot}0$, $\Omega_1 = 2 + 0{\cdot}1\kappa$, the numerical results of the response of equation (1) are shown in Figure 32.

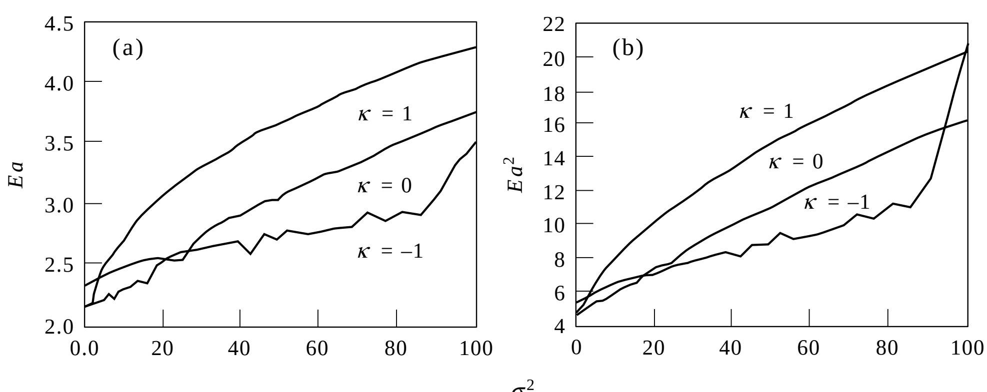

Figure 32. Steady state response of Duffing system: $h_0 = k_0 = 2{\cdot}0$, $\Omega_0 = 2{\cdot}0$. (a) Ea; (b) Ea^2.

7 CONCLUSION

For the first time, the method of multiple scales is used to investigate the principal resonance of a Duffing oscillator to combined deterministic and narrow-band random parametric excitations. Theoretical analyses and numerical simulations show that: (1) When the intensity of the random excitation increases, the trivial steady state solution may lose its stability and the system may have a non-trivial steady state solution. (2) When the intensity of the random excitation increases, the non-trivial steady state solution may change from a limit cycle to a diffused limit cycle. (3) Under some conditions the systems may have two steady state solutions. (4) Under some conditions jumps may exist.

REFERENCES

1. T. T. Soong and M. Grigoriu 1993 *Random Vibration of Mechanical and Structural Systems*. Englewood Cliffs, NJ: Prentice-Hall.
2. R. L. Stratonovitch and Y. M. Romanoviskii 1965 in *Nonlinear Translations of Stochastic Process* (P. T. Kuznetsov, R. I. Stratonovich and V. I. Tikhonov, editors). Oxford: Pergamon. Parametric effect of a random force on linear and nonlinear oscillatory systems.
3. M. F. Dimentberg, N. E. Isikov and R. Model 1981 *Mechanics of Solids* **16**, 19–21. Vibration of a system with cubic-non-linear damping and simultaneous periodic and random parametric excitation.
4. N. S. Namachchivaya 1991 *Journal of Sound and Vibration* **151**, 77–91. Almost sure stability of dynamical systems under combined harmonic and stochastic excitations.
5. S. T. Ariaratnam and D. S. F. Tam 1976 *ZAMM* **56**, 449–452. Parametric random excitation of a damped Mathieu oscillator.
6. M. F. Dimentberg 1988 *Statistical Dynamics of Nonlinear and Time-varying Systems*. New York: Wiley.
7. R. L. Stratonovich 1963 *Topics in the Theory of Random Noise*. New York: Gordon and Breach.
8. S. Rajan and H. G. Davies 1988 *Journal of Sound and Vibration* **123**, 497–506. Multiple time scaling of the response of a Duffing oscillatory to narrow band excitation.
9. A. H. Nayfeh and S. J. Serhan 1990 *International Journal of Nonlinear Mechanics* **25**, 493–509. Response statistics of nonlinear systems to combined deterministic and random excitations.
10. A. H. Nayfeh 1981 *Introduction to Perturbation Techniques*. New York: Wiley.
11. M. Shinozuka 1971 *Journal of Sound and Vibration* **49**, 357–367. Simulation of multivariate and multidimensional random processes.
12. V. I. Oseledec 1968 *Transaction of the Moscow Mathematical Society* **19**, 197–231. A multiplicative ergodic theorem, Lyapunov characteristic numbers for dynamical systems.
13. Fang Tong 1995 *Engineering Random Vibration*. Beijing: Gou Fang Gong Ye Press.